Naval Research Laboratory

Washington, DC 20375-5320

NRL/MR/6390--11-9338

Ground State Resonance Structure of Molecular Clusters of β–HMX Calculated by Density Functional Theory for THz Frequencies

L. Huang

Center for Computational Materials Science
Materials Science and Technology Division

A. Shabaev

George Mason University
Fairfax, Virginia

S.G. Lambrakos

Center for Computational Materials Science
Materials Science and Technology Division

L. Massa

Hunter College
New York, New York

June 21, 2011

REPORT DOCUMENTATION PAGE

Form Approved
OMB No. 0704-0188

1. REPORT DATE *(DD-MM-YYYY)*	**2. REPORT TYPE**	**3. DATES COVERED** *(From - To)*
21-06-2011	NRL Memorandum Report	February 1, 2011 – April 21, 2011

4. TITLE AND SUBTITLE

Ground State Resonance Structure of Molecular Clusters of β-HMX Calculated by Density Functional Theory for THz Frequencies

5a. CONTRACT NUMBER

5b. GRANT NUMBER

5c. PROGRAM ELEMENT NUMBER

6. AUTHOR(S)

L. Huang, A. Shabaev,* S.G. Lambrakos, and L. Massa†

5d. PROJECT NUMBER

5e. TASK NUMBER

5f. WORK UNIT NUMBER

63-0305-01

7. PERFORMING ORGANIZATION NAME(S) AND ADDRESS(ES)

Naval Research Laboratory, Code 6394
4555 Overlook Avenue, SW
Washington, DC 20375-5320

8. PERFORMING ORGANIZATION REPORT NUMBER

NRL/MR/6390--11-9338

9. SPONSORING / MONITORING AGENCY NAME(S) AND ADDRESS(ES)

Office of Naval Research
One Liberty Center
875 North Randolph Street, Suite 1425
Arlington, VA 22203-1995

10. SPONSOR / MONITOR'S ACRONYM(S)

ONR

11. SPONSOR / MONITOR'S REPORT NUMBER(S)

12. DISTRIBUTION / AVAILABILITY STATEMENT

Approved for public release; distribution is unlimited.

13. SUPPLEMENTARY NOTES

*George Mason University, Department of Computation and Data Sciences, Fairfax, VA 22030
†Hunter College, City University of New York, New York, NY 10065

14. ABSTRACT

We present calculations of ground state resonance structure associated with molecular clusters of HMX using density functional theory (DFT), which is for the construction of parameterized dielectric response functions for excitation by electromagnetic waves at compatible frequencies. These dielectric functions provide for different types of analyses concerning the dielectric response of explosives. In particular, these dielectric response functions provide quantitative initial estimates of spectral response features for subsequent adjustment with respect to additional information such as laboratory measurements and other types of theory-based calculations. With respect to qualitative analysis, these spectra provide for the molecular-level interpretation of response structure. The DFT software GAUSSIAN was used for the calculations of ground state resonance structure presented here.

15. SUBJECT TERMS

Density functional theory (DFT) Explosives
Dielectric functions

16. SECURITY CLASSIFICATION OF:			**17. LIMITATION OF ABSTRACT**	**18. NUMBER OF PAGES**	**19a. NAME OF RESPONSIBLE PERSON**
					Samuel G. Lambrakos
a. REPORT	**b. ABSTRACT**	**c. THIS PAGE**	UL	38	**19b. TELEPHONE NUMBER** *(include area code)*
Unclassified	Unclassified	Unclassified			(202) 767-2601

Standard Form 298 (Rev. 8-98)
Prescribed by ANSI Std. Z39.18

Contents

Introduction

A significant aspect of using response spectra calculated by density functional theory, DFT, for the direct construction of dielectric response functions is that it adopts the perspective of computational physics, according to which a numerical simulation represents another source of "experimental" data. This perspective is significant in that a general procedure may be developed for construction of dielectric response functions using DFT calculations as a quantitative initial estimate of spectral response features for subsequent adjustment with respect to additional information such as experimental measurements and other types of theory based calculations. That is to say, for the purpose of simulating many electromagnetic response characteristics of materials, DFT is sufficiently mature for the purpose of generating data complementing, as well as superseding, experimental measurements.

In the case of THz excitation of materials, the procedure of using response spectra calculated using DFT, which is associated with ground state resonance structure, for the direct construction of permittivity functions is well posed owing to the physical characteristic of THz excitation. In particular, it is important to note that the procedure for constructing a permittivity function using response spectra calculated using DFT is physically consistent with the characteristically linear response associated with THz excitation of molecules. Accordingly, one observes a correlation between the advantages of using THz excitation for detection of IEDs (and ambient materials) and those for its numerical simulation based on DFT. Specifically, THz excitation is associated with frequencies that are characteristically perturbative to molecular states, in contrast to frequencies that can induce appreciable electronic state transitions. Of course, the practical aspect of the perturbative character of THz excitation for detection is that detection methodologies can be developed which do not damage materials under examination. The perturbative character of THz excitation with respect to molecular states has significant implications with respect to its numerical simulation based on DFT. It follows then that, owing to the perturbative character of THz excitation, which is characteristically linear, one is able to make a direct association between local oscillations about ground-state minima of a given molecule and THz excitation spectra.

In what follows, calculations are presented of ground state resonance structure associated with molecular clusters of β–HMX. This resonant structure is for the construction of parameterized dielectric response functions for excitation by electromagnetic waves at compatible frequencies. For this purpose the DFT software GAUSSIAN09 (G09) was adopted [1].

The organization of the subject areas presented here are as follows. First, a general review of the elements of vibrational analysis using DFT that are relevant for the calculation of absorption spectra is presented. Second, a general review is presented concerning the formal structure of permittivity functions in terms of analytic function representations. An understanding of the formal structure of permittivity functions in terms of both physical consistency and causality is important for post-processing of DFT calculations for the purpose of constructing permittivity functions. Third, information concerning the ground state resonance structure of molecular clusters of β–HMX, which is obtained using DFT, is presented as a set of case studies. This information consists of the ground state molecular geometry and response spectrum for an isolated molecule. In addition, for each of the explosives, a prototype calculation is presented to demonstrate the construction of parameterized permittivity functions using response spectra calculated using DFT.

Manuscript approved April 22, 2011.

Construction of Dielectric Response Functions using DFT

Density Functional Theory

The application of density functional theory (DFT) and related methodologies for the determination of electromagnetic response characteristics is important for the analysis of parameter sensitivity. That is to say, many characteristics of the electromagnetic response of a given material may not be detectable, or in general, not relevant for detection. Accordingly, sensitivity analyses concerning the electromagnetic response of layered composite systems can adopt the results of simulations using DFT, and related methodologies, to provide realistic limits on detectability that are independent of a specific system design for IED detection. In addition, analysis of parameter sensitivity based on atomistic response characteristics of a given material, obtained by DFT, provide for an "optimal" best fit of experimental measurements for the construction of permittivity functions. It follows that within the context of parameter sensitivity analysis, data obtained by means of DFT represents a true complement to data that has been obtained by means of experimental measurements.

The DFT software GAUSSIAN09 (G09) can be used to compute an approximation of the IR absorption spectrum of a molecule or molecules [1]. This program calculates vibrational frequencies by determining second derivatives of the energy with respect to the Cartesian nuclear coordinates, and then transforming to mass-weighted coordinates at a stationary point of the geometry. [2]. The IR absorption spectrum is obtained using density functional theory to compute the ground state electronic structure in the Born-Oppenheimer approximation using Kohn-Sham density functional theory [3-7]. GAUSSIAN uses specified orbital basis functions to describe the electronic wavefunctions and density. For a given set of nuclear positions, the calculation directly gives the electronic charge density of the molecule, the potential energy *V*, and the displacements in Cartesian coordinates of each atom. The procedure for vibrational analysis followed in GAUSSIAN is that described in [8]. Reference [9] presents a fairly detailed review of this procedure. A brief description of this procedure is as follows.

The procedure followed by GAUSSIAN is based on the fact the vibrational spectrum depends on the Hessian matrix $\mathbf{f}_{\mathrm{CART,}}$ which is constructed using the second partial derivatives of the potential energy *V* with respect to displacements of the atoms in Cartesian coordinates. Accordingly, the elements of the *3N* x *3N* matrix $\mathbf{f}_{\mathrm{CART}}$ are given by

$$f_{\mathrm{CART}ij} = \left(\frac{\partial^2 V}{\partial \xi_i \partial \xi_j} \right)_0 \tag{1}$$

where $\{\xi_1,\xi_2,\xi_3,\xi_4,\xi_5,\xi_6,...,\xi_{3N}\} = \{\Delta x_1,\Delta y_1,\Delta z_1,\Delta x_2,\Delta y_2,\Delta z_2,...,\Delta z_N\}$, which are displacements in Cartesian coordinates, and *N* is the number of atoms. As discussed above, the zero subscript in Eq.(1) indicates that the derivatives are taken at the equilibrium positions of the atoms, and that the first derivatives are zero. Given the Hessian matrix defined by Eq.(1) the operations for calculation of the vibrational spectrum require that the Hessian matrix Eq.(1) be transformed to mass-weighted Cartesian coordinates according to the relation

$$f_{\mathrm{MWC}ij} = \frac{f_{\mathrm{CART}ij}}{\sqrt{m_i m_j}} = \left(\frac{\partial^2 V}{\partial q_i \partial q_j} \right)_0 \tag{2}$$

where $\{q_1,q_2,q_3,q_4,q_5,q_6,...,q_{3N}\} = \left\{\sqrt{m_1}\Delta x_1,\sqrt{m_1}\Delta y_1,\sqrt{m_1}\Delta z_1,\sqrt{m_2}\Delta x_2,\sqrt{m_2}\Delta y_2,\sqrt{m_2}\Delta z_2,...,\sqrt{m_N}\Delta z_N\right\}$ are the mass-weighted Cartesian coordianates. GAUSSIAN computes the energy second derivatives Eq.(2), thus computing the forces for displacement perturbations of each atom along each Cartesian direction. The first derivatives of the dipole moment with respect to atomic positions $\partial\vec{\mu}/\partial\xi_i$ are also computed. Each vibrational eigenmode leads to one peak in the absorption spectrum, at a frequency equal to the

mode's eigenfrequency ν_{n0}. The absorption intensity corresponding to a particular eigenmode *n* whose eigenfrequency is ν_{n0} is given by

$$I_n = \frac{\pi}{3c}\left|\sum_{i=1}^{3N}\frac{\partial\vec{\mu}}{\partial\xi_i}l_{\mathrm{CART}in}\right|^2, \tag{3}$$

where $\mathbf{l}_{\mathrm{CART}}$ is the matrix whose elements are the displacements of the atoms in Cartesian coordinates. The matrix $\mathbf{l}_{\mathrm{CART}}$ is determined by the following procedure. First,

$$\mathbf{l}_{\mathrm{CART}} = \mathbf{M}\mathbf{l}_{\mathrm{MWC}}, \tag{4}$$

where $\mathbf{l}_{\mathrm{MWC}}$ is the matrix whose elements are the displacements of the atoms in mass-weighted Cartesian coordinates and **M** is a diagonal matrix defined by the elements

$$M_{ii} = \frac{1}{\sqrt{m_i}}. \tag{5}$$

Proceeding, $\mathbf{l}_{\mathrm{MWC}}$ is the matrix needed to diagonalize $\mathbf{f}_{\mathrm{MWC}}$ defined by Eq.(2) such that

$$(\mathbf{l}_{\mathrm{MWC}})^{\mathrm{T}}\,\mathbf{f}_{\mathrm{MWC}}(\mathbf{l}_{\mathrm{MWC}}) = \Lambda, \tag{6}$$

where Λ is the diagonal matrix with eigenvalues λ_i. The procedure for diagonalizing Eq.(6) consists of the operations

$$\mathbf{f}_{\mathrm{INT}} = (\mathbf{D})^{\mathrm{T}}\,\mathbf{f}_{\mathrm{MWC}}(\mathbf{D}) \tag{7}$$

and

$$(\mathbf{L})^{\mathrm{T}}\,\mathbf{f}_{\mathrm{MWC}}(\mathbf{L}) = \Lambda, \tag{8}$$

where **D** is a matrix transformation to coordinates where rotation and translation have been separated out and **L** is the transformation matrix composed of eigenvectors calculated according to Eq.(8). The eigenfrequencies in units of (cm^{-1}) are calculated using the eigenvalues λ_n by the expression

$$\nu_{n0} = \frac{\sqrt{\lambda_n}}{2\pi c}, \tag{9}$$

where *c* is the speed of light. The elements of $\mathbf{l}_{\mathrm{CART}}$ are given by

$$l_{\mathrm{CART}ki} = \sum_{j=1}^{3N}\frac{D_{kj}L_{ji}}{\sqrt{m_j}}, \tag{10}$$

where *k, i=1,…, 3N,* and the column vectors of these elements are the normal modes in Cartesian coordinates.

The intensity Eq.(3) must then be multiplied by the number density of molecules to give an absorption strength. It follows that the absorption spectrum calculated by GAUSSIAN is a sum of delta functions whose positions and magnitudes correspond to the vibrational frequencies and magnitudes, respectively. In principle, however, these spectral components must be broadened and shifted to account for anharmonic effects such as finite mode lifetimes and inter-mode couplings.

Dielectric Response Functions

The general approach of constructing permittivity functions according to the best fit of available data for given material corresponding to many different types of experimental measurements has been typically the dominant approach. The present study extends this approach in that calculations of electromagnetic response based on DFT are also adopted as data for construction of permittivity functions. The inclusion of this type of information is significant for accessing what spectral response features at the molecular level are actually detectable with respect to a given set of detection parameters. Accordingly, permittivity functions having been constructed using DFT calculations provide a quantitative correlation between macroscopic material response and molecular structure. Within this context it is not important that the permittivity function be quantitatively accurate for the purpose of being adopted as input for system simulation. Rather, it is important that the permittivity function be qualitatively accurate in terms of specific dielectric response features for the purpose of sensitivity analysis, which is relevant for the assessment of absolute detectability of different types of molecular structure with respect to a given set of detection parameters. That is to say, permittivity functions that have been determined using DFT can provide a mechanistic interpretation of material response to electromagnetic excitation that could establish the well posedness of a given detection methodology for detection of specific molecular characteristics. Within the context of practical application, permittivity functions having been constructed according to the best fit of available data would be "correlated" with those obtained using DFT for proper interpretation of permittivity-function features. Subsequent to establishment of good correlation between DFT and experiment, DFT calculations can be adopted as constraints for the purpose of constructing permittivity functions, whose features are consistent with molecular level response, for adjustment relative to specific sets of either experimental data or additional molecular level information.

The construction of permittivity functions using DFT calculations involves, however, an aspect that requires serious consideration. This aspect concerns the fact that a specific parametric function representation must be adopted. Accordingly, any parametric representation, i.e., parameterization, adopted for permittivity-function construction must be physically consistent with specific molecular response characteristics, while limiting the inclusion of feature characteristics that tend to mask response signatures that may be potentially detectable.

In principle, parameterizations are of two classes. One class consists of parameterizations that are directly related to molecular response characteristics. This class of parameterizations would include spectral scaling and width coefficients. The other class consists of parameterizations that are purely phenomenological and are structured for optimal and convenient best fits to experimental measurements. A sufficiently general parameterization of permittivity functions is given by Drude-Lorentz approximation [10]

$$\varepsilon(\nu) = \varepsilon'(\nu) + i\varepsilon''(\nu) = \varepsilon_\infty + \sum_{n=1}^{N} \frac{\nu_{np}^2}{(\nu_{no}^2 - \nu^2) - i\gamma_n \nu} \ , \tag{11}$$

where ν_{np} and γ_n are the spectral scaling and width of a resonance contributing to the permittivity function. The permittivity ε_∞ is a constant since the dielectric response at high frequencies is substantially detuned from the probe frequency. The real and imaginary parts, $\varepsilon_r(\nu)$ and $\varepsilon_i(\nu)$, respectively, of the permittivity function can be written separately as

$$\varepsilon_r(\nu) = \varepsilon_\infty + \sum_{n=1}^{N} \frac{\nu_{np}^2(\nu_{no}^2 - \nu^2)}{(\nu_{no}^2 - \nu^2)^2 + \gamma_n^2 \nu^2} \quad \text{and} \quad \varepsilon_i(\nu) = \sum_{n=1}^{N} \frac{\nu_{np}^2 \gamma_n \nu}{(\nu_{no}^2 - \nu^2)^2 + \gamma_n^2 \nu^2} \ . \tag{12}$$

With respect to practical application, the absorption coefficient α and index of refraction n_r, given by

$$\alpha = \frac{4\pi\nu}{\sqrt{2}}\left[-\varepsilon_r + \sqrt{\varepsilon_r^2 + \varepsilon_i^2}\right]^{1/2} \quad \text{and} \quad n_r = \frac{1}{\sqrt{2}}\left[\varepsilon_r + \sqrt{\varepsilon_r^2 + \varepsilon_i^2}\right]^{1/2}, \tag{13}$$

respectively, provide direct relationships between calculated quantities obtained by DFT and the "conveniently measurable" quantities α and n_r. It is significant to note that in what follows, the absorption coefficient α is determined using DFT calculated spectra in the same spirit as for its measurement in the laboratory. Although permittivity functions $\varepsilon(\nu)$ are not determined explicitly in the present study, it must be kept in mind that the ultimate construction of these functions is necessary for using DFT calculated spectra to model the dielectric response of complex composite materials and associated detector designs [11].

Ground State Resonance Structure of Molecular Clusters of β–HMX

In this section are presented the results of computational experiments using DFT concerning molecular clusters of β–HMX. These results include the relaxed or equilibrium configuration of a single isolated molecule of β–HMX (see Table 1) and ground-state oscillation frequencies and IR intensities for this configuration, which are calculated by DFT according to the frozen phonon approximation (see Table 2). The ground state resonance structure for a single isolated molecule of β–HMX is adopted as a reference for analysis of spectral features associated with molecular clusters of different sizes. For these calculations geometry optimization and vibrational analysis was effected using the DFT model B3LYP [12, 13] and basis function 6-311G(2d,2p) [14,15]. According to the specification of this basis function, (2d,2p) designates polarization functions having 2 sets of d functions for heavy atoms and 2 sets of p functions for hydrogen atoms [16]. A schematic representation of the molecular geometry of a single isolated molecule of β–HMX is shown in Fig.(1). A schematic representation of molecular geometries of molecular clusters consisting of 3, 5, 7 and 9 molecules are shown in Figs. (2), (3), (4) and (5), respectively. It is significant to note that the relative positions of the molecules associated with each of the molecular clusters is according to crystallographic structure conditions that would be associated with bulk material. In particular, the crystal structure of β–HMX was investigated by Choi and Boutin [17]. The reference code for this crystal structure within the CCDC (Cambridge Crystallographic Data Centre) is OCHTET12. The space group associated with this crystal structure is $P2_1/c$ (symmetry operators are x, y, z; -x, ½+y, ½-z; -x, -y, -z and x, ½-y, ½+z). The unit cell constants ($a = 6.540$ Å, $b =$ 11.050 Å, $c =$ 8.700 Å, $\beta =$ 124.30°) are given by Eiland and Pepinsky [18]. The ground-state oscillation frequencies and IR intensities for the different molecular clusters of β–HMX, corresponding to their relaxed equilibrium configurations, are calculated by DFT according to the frozen phonon approximation. In the cases of molecular clusters of 3, 5 and 7 molecules, these values are given in Tables 3, 4 and 5, respectively. The DFT model and basis function used for these calculations are the same as those used for the single isolated molecule of β–HMX. In the case of 3-molecule clusters, a total of 246 frequencies (from 0 to 3215 cm^{-1}) were calculated (see Table 3). In the case of 5-moleculre clusters a total of 414 frequencies (from 0 to 3203 cm^{-1}) were calculated (see Table 4). In the case of 7-molecule clusters a total of 582 frequencies (from 0 to 3215 cm^{-1}) were calculated (see Table 5). Finally, in the case of 9-molecule clusters the calculated frequencies and IR intensities are given in Table A1 of the appendix.

Discussion

The DFT calculated absorption spectra given in tables 2 to 5 and table A1 provide information for analysis of dielectric response with respect to the size of molecular clusters, i.e., the denumeration of ground state resonance modes and estimates of molecular level dielectric response structure. The construction of permittivity functions using the DFT calculated absorption spectra follows the same procedure as that applied for the construction of permittivity functions using experimentally measured absorption spectra, but with the addition of certain constraint conditions. Accordingly, construction of permittivity functions using either DFT or experimentally measured absorption spectra requires parameterizations that are in terms of physically consistent analytic function representations such as the Drude-Lorentz model, i.e., Eqs.(11) and (12). Although the formal structure of permittivity functions constructed using DFT and experimental measurements are the same, their interpretation with respect to parameterization is different for each case.

Table 1. Atomic positions of β–HMX (Å) after geometry optimization.

Atomic number	X	Y	Z	Atomic number	X	Y	Z
8	-2.479112	0.808262	-3.020958	7	-0.07341	-1.387792	0.284398
8	-3.388653	-0.748745	-1.789495	7	0.84757	-2.298077	-0.230144
8	-0.562157	2.824754	1.293043	6	-0.230216	0.756036	-1.562353
8	-1.864476	2.458008	-0.425286	6	-1.336694	-1.24711	-0.390367
8	2.479112	-0.808262	3.020958	6	0.230216	-0.756036	1.562353
8	3.388653	0.748745	1.789495	6	1.336694	1.24711	0.390367
8	0.562157	-2.824754	-1.293043	1	0.707094	0.321983	-1.911618
8	1.864476	-2.458008	0.425286	1	-0.585747	1.484863	-2.287392
7	-2.458383	-0.034644	-2.142016	1	-1.644269	-2.203497	-0.804192
7	-1.252463	-0.269474	-1.491636	1	-2.080295	-0.92493	0.340903
7	0.07341	1.387792	-0.284398	1	-0.707094	-0.321983	1.911618
7	-0.84757	2.298077	0.230144	1	0.585747	-1.484863	2.287392
7	2.458383	0.034644	2.142016	1	1.644269	2.203497	0.804192
7	1.252463	0.269474	1.491636	1	2.080295	0.92493	-0.340903

Before proceeding with further discussion concerning various features of dielectric response with respect to the size of molecular clusters, it is necessary to again indicate two general goals underlying the DFT calculations presented here and in related studies. These goals are, first, to obtain an understanding of the physical nature underlying the various spectral features associated with the dielectric response of materials, and second, the construction of dielectric response functions for use in quantitative simulation of detector designs and their associated detection scenarios. With respect to the second goal, the DFT calculated absorption spectra given above are to be considered the results of computational experiments for the purpose of being correlated, as well as combined, with other absorption spectra, which may be the results of both computational experiments and laboratory measurements. Accordingly, the dielectric response of a molecular cluster consisting of a given number of molecules can be associated with response features that are intermediate between that of isolated molecules and that of the bulk lattice response. It follows that for analysis of spectra, permittivity functions for finite size molecular clusters can be adopted for use in effective medium theories in order to model the dielectric response of composite materials. This follows in that a composite material may

be characterized by a non-interacting uniform distribution of finite-size molecular clusters within a host material. Models based on this type ofcharacterization are for further investigation.

Proceeding, shown in Figs. 6, 7, 8, 9 and 10 are calculated IR intensities for single isolated molecule, 3-molecule cluster, 5-molecule cluster, 7-molecule cluster and 9-molecule cluster, respectively. We must point out the existence of a mathematical problem associated with the geometry of the 7-molecule cluster. The mathematical criterion of a true minimum in the geometrical energy surface is that the associated vibrational frequencies must all be positive. For the 3-, 5- and 9-molecule clusters, we found configurations corresponding to one of the true minima. For the 7-molecule cluster, however, when optimization was achieved and a stationary point was found, the 7-molecule cluster geometry reported was found to have one negative frequency, although it was of relatively small magnitude (-10.4 cm^{-1}). An extensive search over the geometry surface has not furnished an alternative geometry removing the one negative frequency. Therefore, we are reporting this geometry as our best present estimate for the 7-molecule cluster because it seems to conform to the geometrical trends displayed by the entire series of n-molecule clusters of which it is a part.

Two programs, ConQuest and Mercury [19], have been used for searching the Cambridge Structural Database (CSD), visualizing database entries, HMX, and creating the n-molecule clusters. We have considered the interactions and forces between the single molecule and its neighborhood when we created the cluster. Hydrogen bonding between the molecules is important for establishing the cluster.

Referring to Figs. 6, 7, 8, 9 and 10, one notes continuous spectra consisting of a superposition of essentially Lorenzian functions of various heights and widths, which have been constructed using discrete spectra. Although the primarily purpose of this type of construction within GAUSSIAN is for the purpose of enhanced visualization of spectral features, it is significant to note that this operation represents an estimation of the characteristic scaling and width of resonances contributing the dielectric response. With respect to the interrelationship between the absorption coefficient α and the permittivity function $\varepsilon(\nu)$ defined by Eqs.(11), (12) and (13), this represents an estimation of the parameters ν_{np} and γ_n, which are the spectral scaling and width of a resonance contributing to the permittivity function. For qualitative comparison of spectral features this type of estimate should be sufficient. For the construction of permittivity functions using DFT calculated spectra for subsequent use for quantitative simulation, it is more appropriate, however, to assume the parameters ν_{np} and γ_n adjustable, i.e., to be assigned values according to additional information. This point will be further elucidated below [11].

A qualitative comparison of spectral features is shown in Fig. 11. Referring to Fig. 11(A), it can be observed that in general each molecular cluster is characterized by a relatively distinct spectrum consisting of its own set of characteristic features. Again, hypothesizing with respect to using this type information for construction of models using effective medium theory, a composite material could be characterized by a non-interacting uniform “weighted” distribution of finite-size molecular clusters within a host material, where the weighting is according to the relative fraction of clusters within the distribution consisting of a given number of molecules.

Again referring to Fig.11(A), initial consideration is given to what extent various average features of the DFT calculated spectra for different size molecular clusters, as well as experimentally measured spectra, may be correlated with each other. Referring to Fig. 11(B), it can be seen that on average there exist a noticeable correlation between DFT calculated spectra for 7- and 9-molecule clusters of β–HMX and experimentally measured spectrum for dielectric response of β–HMX in bulk lattice. In particular, one can observe a correlation among frequency ranges for accumulation of peaks, which are within the neighborhoods of 3, 6 and 13 THz. The comparison of spectra shown in Fig.11(B) also supports the notion that certain resonance features, which are associated with finite-size molecular clusters, are preserved within clusters of increasing size, as well as in a bulk lattice structure, thus

implying a persistence of these modes after coupling to intermolecular influences. The persistence of certain intramolecular modes, which is irrespective of molecular cluster size, i.e., whether the molecule is isolated, part of a cluster or within a bulk lattice, is demonstrated by comparison of DFT calculated and experimentally measured spectra. Shown in Table 6 is a comparison of DFT calculated frequencies corresponding to three prominent absorptions, at 58.5, 82.2 and 95.4 cm^{-1}, which have been observed experimentally for a bulk lattice [20]. Referring to this table, and Figs. 6-10, one can observe a high correlation between DFT calculated spectra for different cluster sizes and experimentally determined absorption lines at the specific frequencies indicated.

Remark. It is significant to note that the existence of prominent or persistent modes within the spectra of explosive molecules may have important implications concerning the nature of their activation with respect to the release of energy.

Next, we consider what average spectral features can be correlated with the size of a molecular cluster. Referring to Fig.11, which compares both DFT calculated and experimentally measured spectra [21,22], it can be observed that as the size of the cluster increases, there is a relative increase in the presence of resonance structure at lower frequencies. An examination of this trend in spectral features can be made more quantitative by consideration of the discrete delta-function representation of the DFT calculated spectra. Referring to Fig.12, one observes an increase in the number of absorption lines for the 3-molecule cluster relative to the discrete spectrum associated with a single isolated molecule. Again, referring to this figure, it is significant to note that certain spectral features associated with the isolated molecule can be observed to persist within the spectrum for the molecular cluster.

Proceeding with our comparison of spectra, we note that studies have emphasized the observation that calculated spectra corresponding to a single isolated molecule are not strongly correlated with that of the bulk-lattice. In particular, Allis *et al.* [23] have emphasized that calculated spectra for the dielectric response of a bulk lattice are more appropriate of with the use of periodic boundary conditions for representation of intermolecular influences. Relative to this point, however, the DFT calculations of spectra presented here tend to indicate a relatively interesting result, which has implications with respect to both understanding the nature of coupling between inter- and intra-molecular modes for explosives and the use of calculated spectra for modeling dielectric response for practical applications, i.e., simulation of methods for explosives detection. Specifically, the DFT calculated spectra for molecular clusters show progressively higher correlation with that of the bulk with increasing size of the cluster. This supports the notion that far-field coupling of intramolecular modes to intermolecular modes is dominant only within a restricted range of molecular cluster size. In addition, this implies that with respect to the modeling of bulk lattice response for estimating dielectric response, for the purpose of simulating detection system, DFT calculated spectra corresponding to molecular clusters should provide a reasonable estimate of bulk dielectric response characteristics.

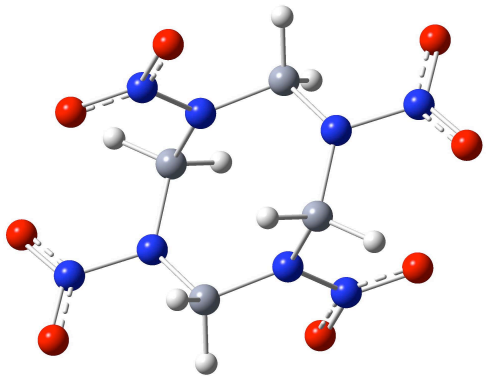

Figure 1. Molecular Geometry of β–HMX.

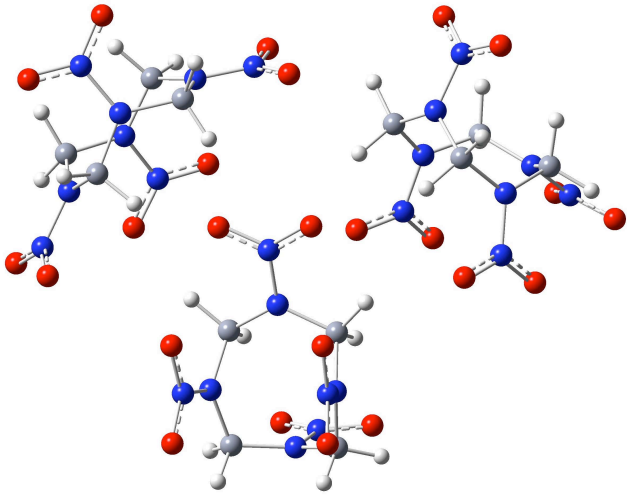

Figure 2. Molecular Geometry of 3-Molecule Cluster of β-HMX.

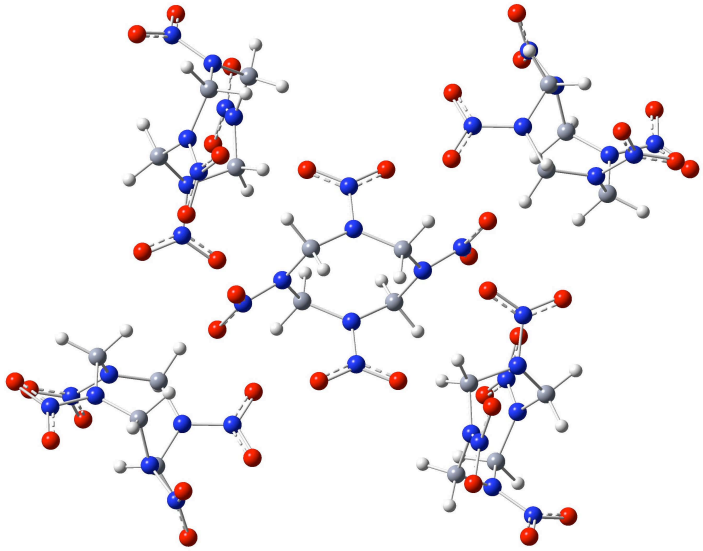

Figure 3. Molecular Geometry of 5-Molecule Cluster of β-HMX.

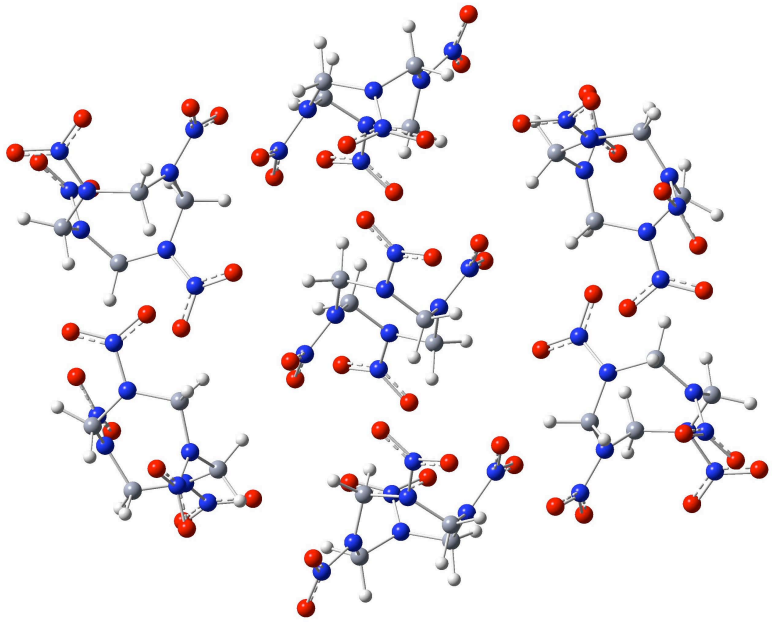

Figure 4. Molecular Geometry of 7-Molecule Cluster of β-HMX.

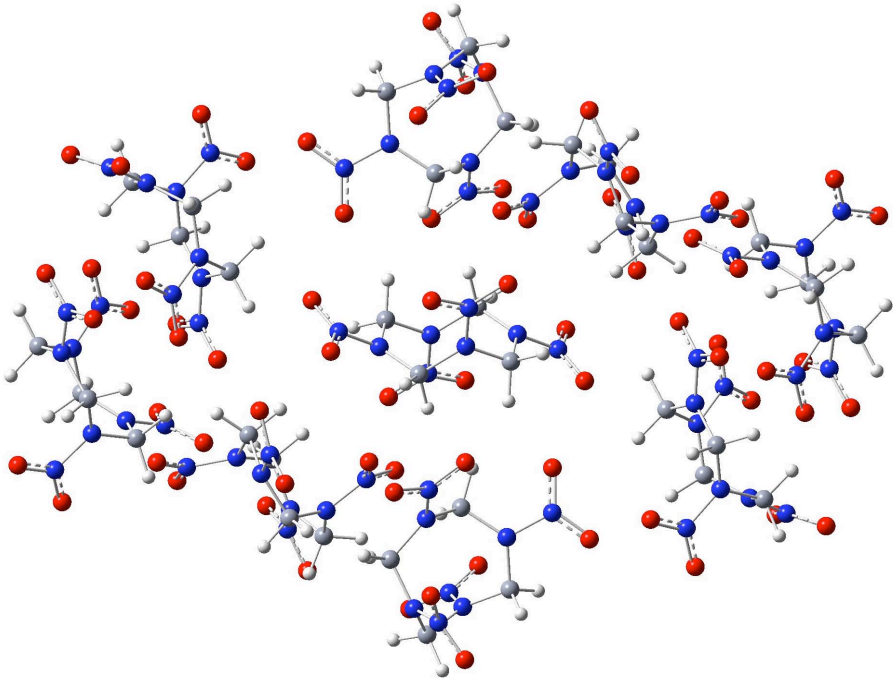

Figure 5. Molecular Geometry of 9-Molecule Cluster of β-HMX.

Table 2. Oscillation frequencies and IR intensities for single isolated molecule of β–HMX.

Frequency cm^{-1}	Intensity (km/mol)	Frequency cm^{-1}	Intensity (km/mol)	Frequency cm^{-1}	Intensity (km/mol)	Frequency cm^{-1}	Intensity (km/mol)
18.0302	3.8738	424.2884	0	963.0203	0	1436.4362	27.8791
53.2212	6.4573	427.9083	5.1902	963.9386	225.5511	1455.2174	0
61.9072	0	600.8529	0	1088.4111	127.2236	1477.3986	0
67.1865	1.4375	603.1155	33.7774	1092.0485	0	1479.2684	39.9261
68.4887	0	633.4601	32.6639	1164.1815	174.3309	1491.2864	0
91.4604	0	638.6084	0	1198.3514	0	1494.7878	105.2168
97.0024	0.2151	656.8692	9.2653	1231.2358	0	1657.0037	0
119.4615	0	661.8475	0	1245.8247	154.3702	1662.1891	512.3396
130.1859	0.583	738.4334	0	1269.5238	54.6922	1670.6206	0
162.0471	0	768.5782	15.3857	1270.5952	0	1671.9207	565.9194
167.7281	10.0649	774.3588	0	1309.1761	0	3076.7251	0
211.0685	18.8994	781.8836	24.3877	1317.175	890.8273	3077.9143	8.8042
221.0217	0	781.9183	0	1331.7427	426.2797	3092.8662	31.2866
272.8039	0	790.6682	19.2817	1343.2512	0	3093.2776	0
300.6558	0	849.4091	0	1356.3191	16.898	3160.9194	0
342.0961	7.5711	849.4226	3.315	1357.3042	0	3161.0083	6.5753
352.9131	0	884.5014	17.3546	1380.5103	14.4161	3164.052	5.613
377.2932	6.7134	896.0556	0	1380.9347	0	3164.2056	0
405.6983	0	951.5063	257.8989	1402.7491	0		
407.3339	5.8638	952.4117	0	1429.9025	57.348		

Table 3. Oscillation frequencies and IR intensities for 3-Molecule Cluster of β–HMX.

Frequency cm^{-1}	Intensity (km/mol)	Frequency cm^{-1}	Intensity (km/mol)	Frequency cm^{-1}	Intensity (km/mol)	Frequency cm^{-1}	Intensity (km/mol)
7.9879	0.0985	161.4394	0.1057	607.3711	40.3292	873.0017	10.5475
11.3529	1.2416	166.0544	0.6321	610.0159	30.0824	873.7899	0.0757
15.6403	0.1418	182.5523	0.5504	614.1347	4.0066	883.1056	2.2741
16.4809	0.1586	185.8211	0.4371	614.7015	6.6024	883.2583	14.3427
18.3337	3.564	191.6799	0.2509	620.8165	40.5581	884.4497	9.8405
19.2346	0.3355	200.7262	10.0067	622.5088	62.2002	902.1969	18.1491
24.7728	0.2454	216.3699	0.8129	627.5184	19.8873	926.1227	242.0018
28.1623	3.2538	220.3405	2.4744	630.0423	17.1819	930.6012	65.6786
31.6222	3.1697	224.3776	0.6027	631.3054	37.4598	934.0608	237.5131
32.82	0.8543	235.2332	0.2952	640.1877	9.0744	939.6913	284.0254
39.3008	2.4282	239.2129	8.058	644.9196	15.4176	942.6224	57.1345
43.5759	4.8667	256.3639	6.419	649.2871	5.141	943.9838	178.9681
48.4647	0.7894	264.0071	9.5621	651.8323	1.7459	949.6719	45.6151
49.5171	3.7659	271.8229	1.0515	667.6313	8.8516	955.4015	301.0852
52.2567	2.386	289.8691	1.4776	677.8409	1.4945	958.7363	4.735
55.018	1.2363	327.4869	3.1593	684.5927	2.8598	962.0817	4.2194
58.5555	1.449	330.2296	3.1677	728.8889	11.6619	970.9299	81.7037
59.6752	2.9624	338.4593	4.8345	734.4506	6.2967	1002.4167	9.7992
69.8108	0.1268	345.89	3.9607	741.8621	9.0287	1034.292	77.1355
70.3625	0.6932	361.1152	0.4893	746.3852	2.8871	1037.2616	222.695
74.4877	2.846	373.7739	0.2923	748.6535	4.8887	1066.2065	20.4679
77.0543	3.283	385.7724	3.4765	765.0253	0.876	1113.8621	29.2814
82.2803	4.4389	391.3591	3.849	768.0635	4.235	1116.4669	54.7688
85.1295	0.1837	397.0634	7.0627	769.6793	2.4005	1119.1401	55.5997
87.6185	1.584	399.9766	4.4436	772.7515	15.534	1122.9521	54.2236
92.1575	1.0529	404.5198	8.5257	773.6643	18.1609	1130.6136	32.8452
95.4647	0.145	405.4004	5.3908	774.6599	14.9173	1168.8269	90.568
99.7255	4.4696	423.8127	5.2313	776.5024	13.6547	1189.8492	14.7302
100.2354	0.677	423.8502	0.617	777.0262	1.9679	1197.1169	14.3981
103.1553	1.0873	428.0997	0.2723	778.3128	11.687	1223.0951	94.0103
104.5185	1.8334	428.5878	6.5864	781.3322	2.6631	1230.2217	31.0365
107.9697	0.6432	431.5572	3.0751	781.8309	8.1711	1238.3191	105.8487
112.0987	1.499	436.8967	15.8708	783.1608	19.9742	1239.4977	16.5671
115.0462	0.4937	443.8386	1.7962	787.037	23.3952	1248.4406	7.3418
120.7019	0.7859	444.8885	1.2628	839.8754	12.8309	1249.6317	43.6042
125.1695	1.1144	450.5671	5.3105	844.2358	6.2762	1250.7643	56.6629
130.2338	0.3324	451.6437	8.1119	846.3209	5.4616	1253.5846	30.6706
137.5823	2.6091	454.0007	2.7235	851.6018	11.2655	1255.548	13.6163
144.3083	1.0261	601.0216	2.4549	861.4545	4.2301	1260.3625	75.5184
153.0266	0.2896	604.3344	18.5732	868.5721	0.7026	1264.0328	147.7119

Table 3. Continued

Frequency cm^{-1}	Intensity (km/mol)	Frequency cm^{-1}	Intensity (km/mol)	Frequency cm^{-1}	Intensity (km/mol)	Frequency cm^{-1}	Intensity (km/mol)
1273.8141	168.4293	1397.4493	36.341	1608.6603	412.0217	3172.75	12.9191
1285.6196	21.5424	1400.5265	2.0401	1621.6316	212.5013	3174.7351	11.3718
1304.5571	571.9207	1416.1903	2.2636	1629.6068	13.9015	3176.1082	6.3768
1305.8774	203.7391	1419.139	52.4575	1646.525	259.3514	3179.988	5.3687
1309.955	475.9932	1422.781	5.5841	1650.1842	466.2529	3180.1074	5.173
1314.322	548.4938	1423.9001	26.6199	1655.1735	265.7855	3181.7358	23.899
1319.0951	325.2185	1431.8574	6.1014	1656.2119	74.437	3181.8621	15.0437
1321.8273	409.5321	1433.05	83.739	1661.0408	47.4949	3183.6387	11.9819
1322.3409	212.9034	1433.9814	3.4809	1664.5782	121.7169	3205.8923	24.0908
1325.5502	112.9019	1435.3016	69.2356	1665.3721	564.2691	3207.7437	28.8292
1333.4797	306.2935	1454.2489	37.5631	1673.3284	516.6258	3215.1382	27.009
1343.2627	4.1515	1454.894	52.4266	1682.0833	292.0001		
1346.923	9.1548	1466.3292	0.3485	3080.4905	9.7041		
1357.0865	61.697	1467.9146	32.446	3081.0762	4.5206		
1360.2462	40.0523	1471.731	28.2125	3083.7827	4.5466		
1364.3752	94.7469	1475.3832	14.7345	3096.1189	0.8583		
1366.5074	155.45	1481.3087	99.2865	3098.3938	17.7271		
1366.903	212.3928	1481.9788	7.3134	3103.9734	0.8933		
1369.4558	52.5194	1482.6957	27.8891	3111.3213	1.064		
1371.8492	83.4915	1484.5076	83.2644	3112.3047	9.7653		
1382.0085	3.156	1488.9092	54.6117	3120.752	2.1992		
1383.3636	38.1987	1493.4417	70.7739	3125.1504	2.5162		
1389.4236	5.2728	1496.781	22.6728	3127.9104	2.8401		
1395.2242	2.5155	1498.1814	25.0258	3148.7285	5.2637		
1395.5757	3.3339	1501.021	9.9543	3159.7031	0.1263		

Table 4. Oscillation frequencies and IR intensities for 5-Molecule Cluster of β–HMX.

Frequency cm^{-1}	Intensity (km/mol)	Frequency cm^{-1}	Intensity (km/mol)	Frequency cm^{-1}	Intensity (km/mol)	Frequency cm^{-1}	Intensity (km/mol)
2.4449	1.0118	78.731	0	189.4898	2.0391	436.5072	0
7.9161	0.4769	81.1692	0	196.2481	5.0308	436.9558	19.1666
8.7798	0	82.5976	2.4727	196.3151	0	437.1389	0
9.2942	0.5141	87.129	0	200.5013	0	438.2292	20.6113
11.5725	0	87.2426	0.8253	200.6289	12.8947	442.1407	18.1771
11.6189	1.5707	88.7151	0	213.7244	11.3068	442.1622	0
13.3127	0	88.8132	1.6167	213.8078	0	451.2878	5.3524
13.6872	1.3638	90.6732	3.3363	225.4272	0	451.2907	0
16.2908	0.5299	91.8066	0	232.188	20.3108	455.1775	14.9082
16.8014	0	95.6066	0	283.6123	0	455.1923	0
18.2778	0	96.6886	10.3162	291.3282	0	460.8227	0
21.5271	0.2558	99.6324	0	291.3473	4.301	460.9097	25.9295
23.9791	0	102.8605	3.3954	294.1221	2.9145	461.5491	16.4504
26.4528	3.6673	116.9738	1.2005	294.1317	0	461.8036	0
27.1124	0	117.0753	0	294.4574	5.3094	599.5859	41.4041
27.832	0.7616	119.3919	0	294.4767	0	599.6444	0
28.9961	0	119.9465	3.1452	301.416	0	603.3742	0
30.808	8.4772	120.7225	0	301.4505	1.3247	603.5998	29.1256
32.9547	0	120.791	1.7477	316.9876	0	606.1093	0
38.7325	1.7614	123.9584	0	357.3448	3.0529	608.8617	30.4632
39.1175	0	125.4357	2.1986	357.5127	0	611.931	0
41.8084	2.7525	138.3209	0	358.0236	6.3184	611.9319	54.8976
43.1105	0	140.1593	6.2559	358.2293	0	613.539	0
49.535	0	141.4129	0	360.0048	3.3543	613.6089	42.7628
50.1757	2.3845	143.962	1.1367	366.4901	0	620.1086	0
50.7227	0	144.8766	0	385.058	7.5675	620.1096	8.253
52.0354	4.5907	146.541	0	385.7347	0	621.3665	0
56.3428	0	148.2743	8.1168	390.6185	8.9175	621.3891	16.1136
60.0284	5.311	148.9485	0.1671	391.3114	0	629.7927	0
60.7367	0	171.4106	0	391.5093	10.2552	630.135	87.5523
62.9123	0.5175	171.4603	1.4484	395.4532	8.3463	630.3287	18.033
64.6856	0	171.7756	0	395.4555	0	630.4682	0
65.9255	2.1815	172.1423	0.6174	396.2608	3.762	636.0826	88.5726
66.7811	0	179.2336	4.9422	396.2773	0	642.4485	0
70.6	2.6553	181.3055	0	415.7079	0	645.318	12.1267
70.8454	0	181.9208	0	420.8055	5.4356	645.3838	0
71.9479	0	181.9274	3.7945	422.3565	0	646.2989	15.4838
73.1675	8.6762	183.1067	20.297	422.4878	7.4335	646.3108	0
75.5286	0.8237	188.7956	0	426.0599	0	663.3046	24.5647
77.4352	1.2045	189.4715	0	426.302	4.4419	668.2143	0

Table 4. Continued

Frequency cm^{-1}	Intensity (km/mol)	Frequency cm^{-1}	Intensity (km/mol)	Frequency cm^{-1}	Intensity (km/mol)	Frequency cm^{-1}	Intensity (km/mol)
693.7723	0	853.3085	19.2907	1085.2422	154.3393	1316.8861	605.0174
693.8261	26.3698	853.3218	0	1085.3749	0	1317.9095	0
695.2532	0	859.5745	26.4173	1103.295	80.204	1321.2434	0
695.2812	38.3839	859.6055	0	1109.187	0	1321.5704	557.7111
720.8468	8.4233	879.8152	6.9185	1174.0422	150.95	1328.316	0
720.8659	0	879.8179	0	1179.0529	0	1328.5341	524.9082
722.6338	0	882.8856	23.4293	1179.0918	102.4703	1329.5229	1722.9796
722.6906	4.5474	883.0042	0	1186.7131	118.4736	1332.5619	0
726.056	0	883.9244	8.9853	1186.7213	0	1333.2533	207.5224
726.0613	1.3335	887.6967	0	1191.0179	107.1316	1340.2136	0
727.9267	6.9482	887.7436	29.4219	1191.0302	0	1342.9421	0
727.9734	0	889.7379	0	1191.73	0	1343.4224	121.0959
737.8149	0	889.7539	30.3391	1191.7498	58.4698	1346.6918	0
768.5469	31.6833	897.7753	0	1194.772	59.099	1346.7155	48.2207
770.988	0	930.0012	838.794	1194.8312	0	1347.4851	0
772.446	12.2524	930.4136	0	1198.8754	0	1347.5867	176.8391
772.4625	0	933.9737	0	1198.9727	67.1672	1351.3273	4.9499
772.5678	13.6437	934.0325	170.5281	1201.0917	0	1351.5244	0
772.6995	0	935.5304	0	1231.4447	0	1355.1648	85.1409
772.7476	9.8388	935.6268	418.0584	1239.4788	196.2004	1357.615	0
772.8547	0	936.7015	734.308	1240.005	0	1368.9071	0
773.8651	0	936.8202	0	1242.2606	49.0347	1369.7911	257.9252
773.8676	10.9936	946.9066	98.1032	1242.8459	0	1372.0817	70.0738
778.3443	12.0009	947.2906	0	1243.4779	501.724	1373.533	0
778.7996	0	948.6198	263.297	1254.7036	0	1385.9373	56.0723
782.379	58.0145	949.1339	0	1254.8458	190.3744	1386.7932	0
782.4064	0	960.5663	158.9462	1256.2631	0	1386.9333	17.7201
782.5579	17.6144	962.1402	0	1256.369	138.2537	1388.6195	0
782.6372	0	965.6904	41.7534	1265.0303	95.4435	1388.9382	104.5421
783.5877	38.3302	965.9821	0	1267.4193	0	1392.437	0
783.768	0	970.543	67.1194	1295.3835	281.2031	1395.3827	12.1464
783.8214	32.4982	970.6497	0	1295.4038	0	1395.5607	0
783.926	0	976.3635	0	1300.1277	0	1396.3622	6.8135
788.7197	23.4513	980.3981	184.895	1300.3503	481.2963	1396.4023	0
837.9593	0	1048.1564	72.2374	1302.6163	0	1399.3125	37.2968
838.0296	22.3987	1048.226	0	1302.6423	208.9123	1399.3259	0
841.3698	0	1053.9576	0	1304.2137	0	1400.7384	0
841.3727	16.8682	1054.0659	56.0722	1304.627	217.4059	1400.7443	20.2644
847.8915	8.6864	1083.9583	205.3256	1308.4095	0	1404.4886	0
848.8383	0	1083.96	0	1313.3644	1428.5823	1422.4409	74.0817

Table 4. Continued

Frequency cm^{-1}	Intensity (km/mol)	Frequency cm^{-1}	Intensity (km/mol)	Frequency cm^{-1}	Intensity (km/mol)	Frequency cm^{-1}	Intensity (km/mol)
1422.7311	0	1492.3304	40.2023	1673.3658	0	3140.7634	0
1424.4413	81.2186	1492.3788	0	1673.5356	462.8472	3140.7644	16.0451
1424.4712	0	1493.924	62.6376	1684.4061	0	3154.7715	0
1432.7206	10.1001	1493.9532	0	1684.4677	565.4249	3154.7922	23.7558
1433.3306	0	1494.5437	165.1711	1694.8595	0	3170.9856	0
1433.4095	89.0023	1494.5942	0	1694.9045	663.5389	3170.9858	4.379
1433.7047	0	1496.6158	12.9397	3083.4172	0	3177.9053	190.0601
1434.4045	124.7351	1496.6851	0	3083.438	7.7015	3178.1794	0
1445.585	55.8381	1506.903	0	3086.4121	0	3179.3699	0
1459.0468	0	1510.4193	69.5984	3086.9099	29.5786	3179.3718	0.8514
1459.1266	17.0045	1618.1127	0	3090.9229	0	3181.365	0
1460.9264	0	1619.5496	496.1726	3090.9263	2.7171	3181.3672	16.2667
1460.9865	21.6195	1624.1208	177.7645	3098.8635	17.0408	3191.6733	6.6494
1464.0145	0	1624.8184	0	3098.8916	0	3191.6794	0
1464.3307	37.252	1631.3607	0	3109.1179	3.7435	3194.5439	0
1464.8092	0	1636.0029	963.9075	3109.1191	0	3194.5452	11.9351
1468.1937	33.4104	1639.2675	0	3111.7795	1.2016	3196.3547	34.2831
1468.2087	0	1640.4634	479.8561	3111.7825	0	3196.3667	0
1481.5265	0	1646.0341	0	3116.5728	0	3201.6001	13.0938
1481.8577	170.047	1646.3195	847.6317	3116.592	81.9352	3201.6021	0
1485.6362	0	1660.6912	225.6659	3123.8525	0	3203.4043	51.8636
1486.2424	122.4639	1660.7242	0	3123.8533	0.8645	3203.4314	0
1487.1587	0	1666.222	0	3126.7288	0		
1488.863	36.0715	1666.3921	700.9376	3126.731	15.3074		

Table 5. Oscillation frequencies and IR intensities for 7-Molecule Cluster of β–HMX.

Frequency cm^{-1}	Intensity (km/mol)	Frequency cm^{-1}	Intensity (km/mol)	Frequency cm^{-1}	Intensity (km/mol)	Frequency cm^{-1}	Intensity (km/mol)
-10.4206	0.2726	56.5432	3.7121	122.6403	0	228.4549	37.9412
5.0661	0.197	59.1242	6.8862	122.694	0.036	228.668	0
6.9366	0.5308	60.6233	0.7608	127.2126	0	230.0808	6.1599
9.073	0	61.0188	0	127.9785	0.3749	235.6238	0
11.8335	0.1208	62.2131	1.5588	129.0463	0	235.7752	11.5904
12.0545	0	64.2215	0	129.6631	3.9117	238.6877	0
13.4439	0	65.1673	0	130.9912	5.2257	273.1025	0
14.585	4.6752	66.1939	6.2853	131.7566	0	273.1572	0.822
16.4632	1.7042	69.8698	0	132.7578	0	283.9046	0
17.6956	0	69.9812	4.3281	132.8398	1.1662	284.6883	0.948
19.8383	0	75.0556	3.6883	135.1802	0	285.021	0
20.2965	0.6367	75.7598	0	135.3666	3.4052	288.7714	3.5853
21.0133	0.4545	81.4765	0	138.4739	0	288.7743	0
22.9016	0	81.6776	0.5593	138.7251	2.472	297.6727	0
24.0237	0	86.1546	9.1869	143.5806	0	297.7986	11.814
24.888	0	86.7179	0	144.6877	0.1251	303.5629	3.6874
25.4518	0.3572	88.2722	0	147.0282	0	303.5928	0
26.2653	0	88.7386	5.9054	149.3198	1.4748	307.6038	0
26.6212	0.6786	91.5378	0	154.1875	8.085	307.6417	1.0313
30.8546	0	92.3833	0.7765	154.2044	0	314.0014	0
31.6454	2.5704	92.882	0	155.5295	0.7132	353.5082	11.7806
32.1753	0.4625	94.1775	0.808	155.6768	0	353.5455	0
32.4892	0	95.0317	0	166.5959	0	354.7209	0
32.6703	0	97.2217	3.733	166.6702	0.3537	354.7473	16.7247
34.6019	0	98.4352	0	169.5334	0	361.7011	3.5645
35.5254	6.4913	99.5276	7.3155	170.5935	1.6529	361.7316	0
38.5586	0	103.3749	1.2772	172.0691	0	362.3772	1.4128
39.3027	13.175	104.4198	5.1722	180.5257	12.3296	362.3862	0
40.9056	0	104.4412	0	185.9353	0	365.7009	3.1917
41.6091	1.2521	105.4396	0	185.9594	6.7863	371.927	0
44.4832	1.7298	105.9665	11.7493	192.11	0	372.7201	1.0947
45.1585	0	106.0478	0	192.2289	6.9386	372.7273	0
45.7918	2.787	106.8942	6.2128	195.964	0	374.2417	2.6248
46.3955	0	111.1651	0	196.0115	1.1298	374.4291	0
48.6612	5.0163	114.4014	5.1772	198.41	18.2705	390.5442	12.0411
49.5348	0	115.071	0	198.654	0	399.1409	0
49.9775	5.3234	115.9726	5.3009	200.0251	0	399.1667	3.0151
50.6288	0	116.0669	0	200.123	18.1689	401.3999	9.0482
51.8515	2.3068	119.4868	1.0398	219.3035	0	401.44	0
53.3338	0	611.1912	45.3419	739.865	0	839.3477	0
405.5521	0						

Table 5. Continued

Frequency cm^{-1}	Intensity (km/mol)	Frequency cm^{-1}	Intensity (km/mol)	Frequency cm^{-1}	Intensity (km/mol)	Frequency cm^{-1}	Intensity (km/mol)
405.5896	12.8583	611.2975	0	742.1831	11.3965	839.369	11.5238
412.9465	24.4828	613.6347	0	742.1846	0	847.7339	9.956
413.0406	0	613.6996	81.1368	759.7083	4.4609	849.4666	0
414.2312	9.3492	618.0961	0	759.7147	0	868.7652	21.711
414.232	0	618.1036	20.3587	766.2378	42.0691	868.7846	0
420.458	0	621.6579	0	768.0605	0	869.41	0
426.1246	0	621.7319	39.1036	768.2879	15.5174	869.4287	22.1147
426.1372	3.328	626.5864	59.7928	770.4546	0	875.1939	23.0756
429.4442	7.5413	626.6224	0	770.4989	10.9872	875.2202	0
429.9361	0	628.7706	28.5396	772.8878	0	879.2352	17.658
430.6698	12.089	628.7857	0	772.9388	15.5954	879.2363	0
433.2759	0	629.8195	0	774.2505	0	881.6051	8.3301
433.6832	5.9361	629.9482	95.4691	774.3417	15.0677	881.6164	0
435.4506	0	638.6975	0	774.4615	0	883.331	19.7572
435.5366	13.1231	640.0414	24.2389	774.5543	25.3102	883.3648	0
436.781	0	647.7834	0	775.2086	56.5431	884.0571	7.6565
437.087	6.2041	647.8108	6.5331	775.2798	0	886.6979	0
445.3145	1.5013	648.2346	0	775.7667	0	886.807	41.0646
445.3334	0	648.2391	9.1348	775.8447	29.5429	897.2648	0
445.9723	0	649.2656	45.4318	776.0028	0	902.8389	44.042
445.9764	2.6137	649.3006	0	777.3285	0	902.9592	0
448.9739	21.3359	650.4223	11.2727	777.3306	26.154	920.2416	0
450.7472	0	650.4343	0	780.4724	44.9349	920.2682	357.7807
459.6847	6.0432	669.3944	16.6654	781.2497	0	923.4285	254.9193
459.7267	0	669.7517	0	781.807	43.6368	923.465	0
463.8357	0	671.3572	30.9827	782.0147	0	933.0518	0
463.8452	12.8939	675.496	0	782.7372	51.4853	934.0133	532.2123
467.4187	21.6096	688.5546	51.758	782.8699	0	934.6809	320.5152
467.4227	0	688.6698	0	783.5379	51.4462	935.0029	0
596.9921	0	702.7462	0.2638	783.6517	0	937.9259	429.77
597.0409	28.0478	702.7476	0	783.7687	36.9918	938.4881	0
600.9204	48.6664	713.6974	0	786.6418	0	944.9778	279.2268
601.0566	0	713.711	18.0131	786.6561	49.7097	945.084	0
601.6047	0	724.0152	0	830.2538	0	951.1747	0
602.7995	22.6543	724.2454	7.3601	830.2867	37.5251	951.2208	162.4113
602.8529	0	734.3072	0	835.4735	0	954.2618	0
606.1879	31.2093	734.527	12.547	835.4902	33.9066	954.2746	108.8956
606.7286	0	737.3613	0	838.7024	23.4603	956.0842	0
609.8161	153.8237	739.7784	14.5182	838.8157	0	957.7764	75.2776
960.0128	289.942	1211.8896	0	1326.5796	0	1399.1234	0

Table 5. Continued

Frequency cm^{-1}	Intensity (km/mol)	Frequency cm^{-1}	Intensity (km/mol)	Frequency cm^{-1}	Intensity (km/mol)	Frequency cm^{-1}	Intensity (km/mol)
960.9496	0	1212.0178	199.4128	1327.0426	553.2102	1399.1379	26.3419
964.4737	187.2417	1217.4529	0	1329.5571	1257.5035	1400.4515	41.2116
965.2439	0	1231.6833	78.1278	1329.9282	0	1400.4626	0
970.5487	113.9154	1231.8947	0	1330.5558	803.7852	1404.136	51.9708
970.5648	0	1232.92	129.9004	1331.6246	0	1404.2513	0
975.1622	101.402	1241.3634	0	1333.083	296.0827	1408.8164	13.1448
975.1763	0	1241.4482	154.9081	1334.0583	0	1408.8188	0
1005.4972	0	1249.1139	0	1336.6475	158.1765	1419.3616	0
1005.5024	18.1713	1249.4924	350.4712	1337.2458	0	1422.726	71.3051
1039.8835	0	1250.5638	142.7871	1340.2205	0	1422.8201	0
1040.0081	162.9091	1250.6158	0	1340.498	167.0564	1426.9042	127.226
1056.684	0	1253.2603	0	1341.587	50.9797	1427.3385	0
1056.707	94.662	1253.2681	38.0582	1341.5946	0	1428.9292	0
1061.9913	0	1260.1552	0	1350.1	0	1428.9293	72.5786
1062.1941	54.805	1260.1903	148.1603	1350.2294	175.6411	1429.5284	0
1090.5774	0	1271.1516	234.9478	1352.3901	104.4767	1429.5349	41.9991
1090.7255	259.2252	1271.3762	0	1359.4282	0	1433.475	135.1421
1095.4921	0	1274.2577	151.5646	1361.1012	146.1022	1439.016	17.3127
1095.7401	74.7002	1277.6766	0	1361.5713	0	1439.0424	0
1106.4862	61.403	1279.057	195.3622	1365.6779	324.0192	1439.8466	0
1106.6674	0	1279.1078	0	1366.1523	0	1439.9409	160.8037
1116.3105	0	1284.9919	0	1367.845	199.3444	1447.4233	12.0416
1116.4412	123.2504	1285.0162	25.5503	1368.1971	0	1447.7338	0
1160.2618	239.1468	1289.868	0	1368.573	3.323	1449.6786	6.4462
1164.4036	0	1290.752	74.996	1368.8044	0	1451.9014	97.4419
1165.8405	101.7706	1301.5424	0	1376.368	0	1451.9709	0
1168.1072	40.5733	1301.8405	415.4483	1376.4969	231.4152	1455.6174	0
1168.1232	0	1302.0004	0	1381.2341	45.9451	1455.684	34.234
1175.7551	113.7819	1302.1777	175.6131	1382.7106	0	1460.7944	0
1175.825	0	1305.975	0	1385.6147	0	1461.076	174.4017
1192.0295	0	1308.0491	435.9346	1385.7228	82.495	1461.1316	0
1198.2299	0	1309.2767	0	1387.2542	65.7012	1462.0247	0
1198.3311	84.8259	1309.6953	432.9558	1387.2639	0	1464.4771	5.2224
1201.4093	0	1310.5448	0	1389.7032	111.6434	1464.4875	0
1201.4196	64.4193	1311.1182	856.6191	1390.5645	0	1465.9723	13.816
1202.6082	232.0283	1316.3955	0	1394.0295	73.2519	1466.1931	0
1202.7588	0	1319.0399	1034.1355	1394.3949	0	1466.2134	28.8594
1208.7418	0	1323.3022	0	1397.9597	0	1476.2391	20.4992
1208.7677	145.8378	1323.3344	945.5623	1397.9885	64.6595	1476.2574	0
1478.2188	14.0751	1629.8489	0	3097.7888	0	3162.6299	0

Table 5. Continued

Frequency cm^{-1}	Intensity (km/mol)	Frequency cm^{-1}	Intensity (km/mol)	Frequency cm^{-1}	Intensity (km/mol)	Frequency cm^{-1}	Intensity (km/mol)
1478.2249	0	1634.4243	423.167	3097.7905	2.3957	3162.6299	10.353
1482.7225	0	1641.1504	0	3100.3647	62.4948	3171.3574	0
1482.7844	59.1478	1641.3759	1085.0548	3100.3701	0	3171.3811	94.5409
1484.9667	257.7006	1644.8771	242.1583	3100.801	22.5725	3180.5554	0
1485.3198	0	1646.1697	0	3100.8416	0	3180.5564	22.6075
1489.6838	283.2304	1648.9836	469.1745	3102.5022	0	3180.7595	29.9912
1489.7383	0	1649.5201	0	3102.5054	17.0532	3180.7979	0
1495.3501	0	1659.3031	298.8028	3108.8215	25.3569	3181.7532	0
1496.045	90.8086	1659.3158	0	3108.822	0	3181.7654	71.3126
1496.2155	0	1663.7723	0	3111.5679	0.9418	3186.4712	34.7356
1498.7257	36.5938	1663.792	225.8324	3111.5679	0	3186.4971	0
1498.8698	0	1664.3274	0	3114.5681	0	3189.9382	0
1499.1443	86.8719	1664.525	676.7529	3114.5681	7.2135	3189.9387	16.2935
1501.0909	0	1666.5013	0	3117.4924	0	3192.3813	50.8223
1501.1635	31.5374	1666.8204	1094.89	3117.8203	18.9474	3192.3818	0
1509.9368	0	1682.5144	671.7492	3118.0964	0	3193.5161	0
1510.0027	94.4268	1682.5728	0	3118.0977	2.8543	3193.5198	19.7585
1606.6178	822.2169	1697.0533	0	3124.2949	0	3194.4502	0
1607.1708	0	1697.1653	581.9431	3124.2976	15.8741	3194.4592	45.8783
1611.1364	644.8557	3084.8738	8.8039	3146.7461	1.1744	3202.4663	16.0376
1612.3207	0	3084.8743	0	3146.9502	0	3202.4922	0
1621.0048	289.6107	3086.6372	0	3160.6172	4.6815	3215.1277	0
1621.2532	0	3086.6375	15.884	3160.6213	0	3215.1372	8.964
1626.752	0	3094.269	15.896	3160.7842	40.5399		
1628.2063	220.4467	3094.2725	0	3160.8582	0		

Table 6. Comparison of DFT calculated and experimentally measured frequencies at prominent absorptions.

Experiment	Bulk-HMX	58.5	82.2	95.4
DFT	1-HMX	53.2 (6.4)	-	97 (0.2)
	3-HMX	58-59 (1.4-2.9)	82 (4.4)	99 (4.5)
	5-HMX	60 (5.3)	82.6 (2.5)	96.7 (10.3)
	7-HMX	59.1 (6.9)	86.2 (9.18)	99.5 (7.3)
	9-HMX	57.2 (15.08)	82.5-84 (4.4-5.0)	99 (3.8)

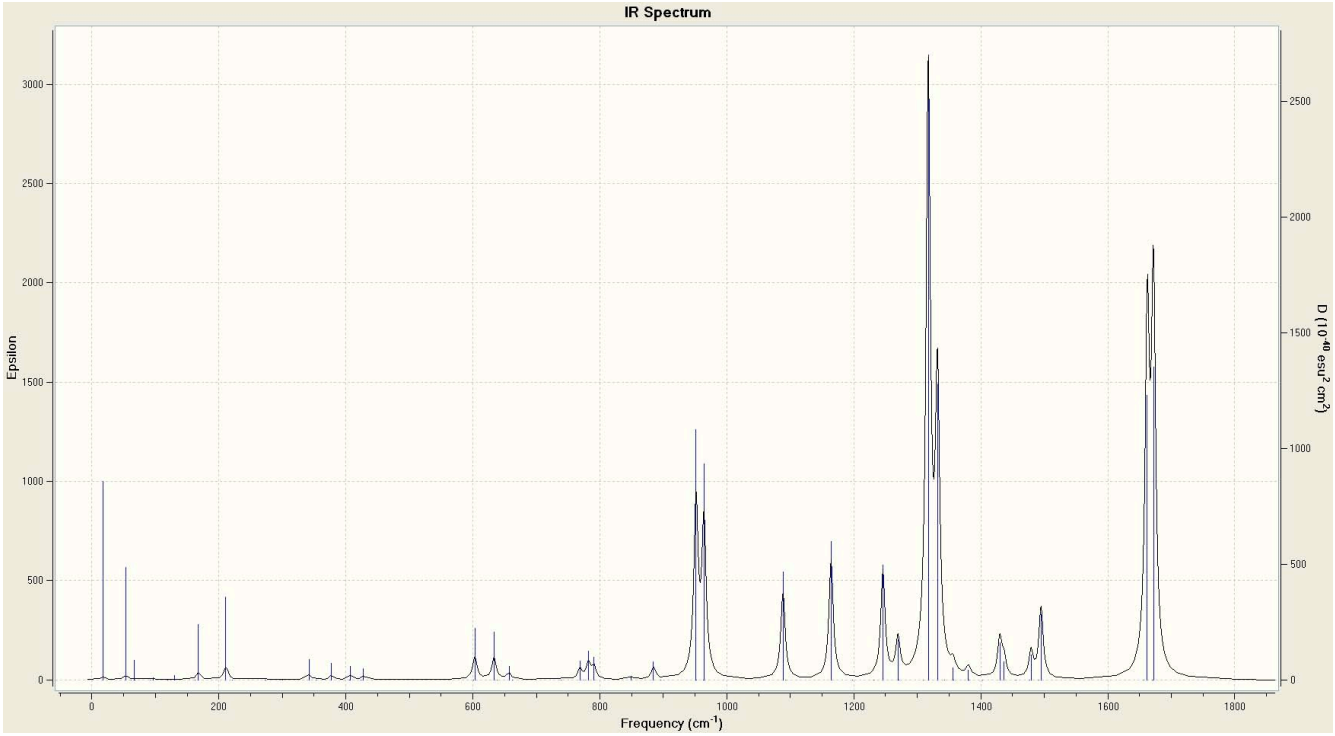

Figure 6. IR intensity as a function of frequency calculated using DFT B3LYP/6-311G(2d,2p) for single isolated molecule of β–HMX according to frozen phonon approximation.

As stated explicitly in the introduction, our goal is the use of DFT for the direct construction of dielectric response functions by adopting the perspective of computational physics, according to which a numerical simulation represents another source of "experimental" data for the purpose of generating data complementing, as well as superseding, experimental measurements. This goal is supported with reference to Figs. 11(A) and 11(B), where it can be seen that there exist non-negligible resonance structure within the region of the spectrum near and below 2 THz as predicted by DFT, while there exist essentially negligible resonance structure as determined by laboratory measurement. For example, referring Fig. 13, as well as reference [20], suggests the possibility that perhaps there exist a limitation of the associated methodologies for measuring the dielectric response of bulk HMX in the spectral region below 2 THz. These observations could also suggest that within this region of the spectrum the molecular cluster model, consisting of 7 or 9 molecules, is no longer an appropriate representation of a bulk system.

Remark. It is important to remember (as discussed above), that the DFT calculated dielectric response functions for molecular clusters of β–HMX presented here, in addition to apparently providing a reasonable representation of bulk response, have potential application for the modeling of gas phase and composite systems consisting of molecular-cluster distributions. That is, composite systems whose basic components include molecular clusters in fact.

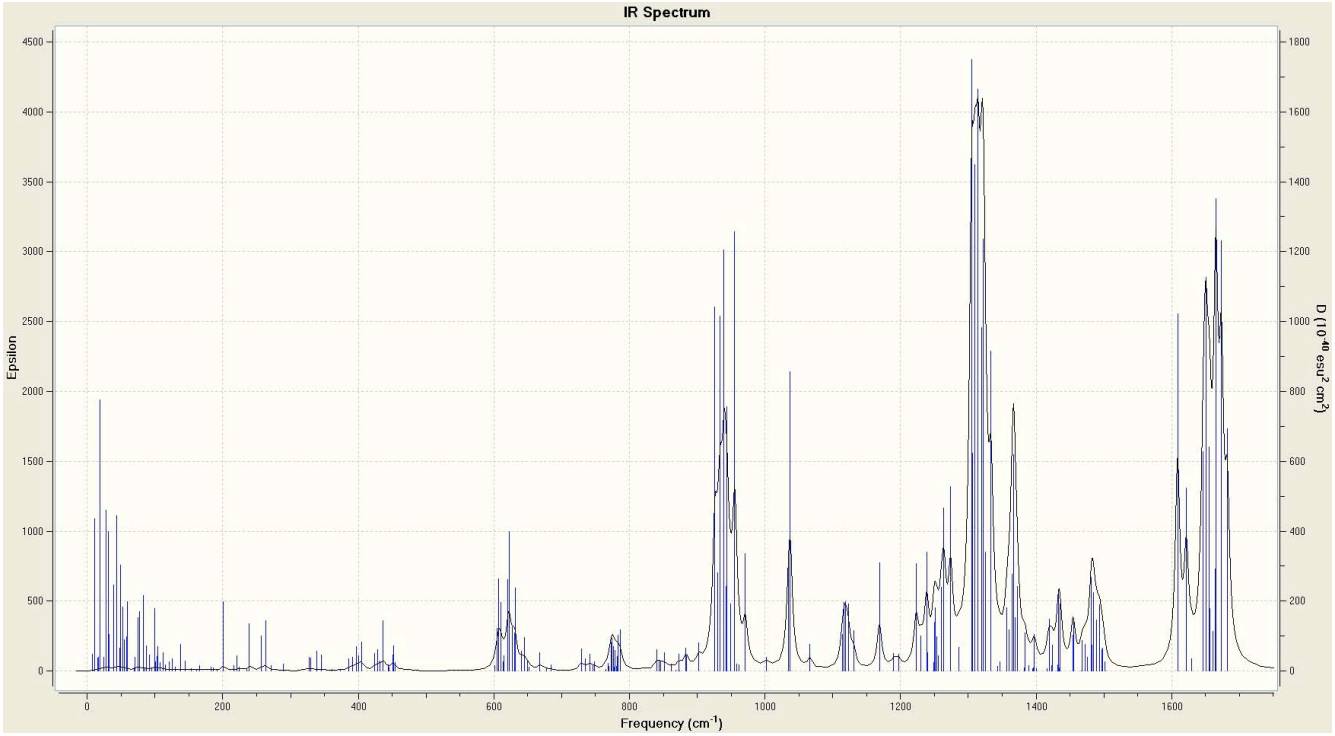

Figure 7. IR intensity as a function of frequency calculated using DFT B3LYP/6-311G(2d,2p) for three-molecule cluster of β-HMX according to frozen phonon approximation.

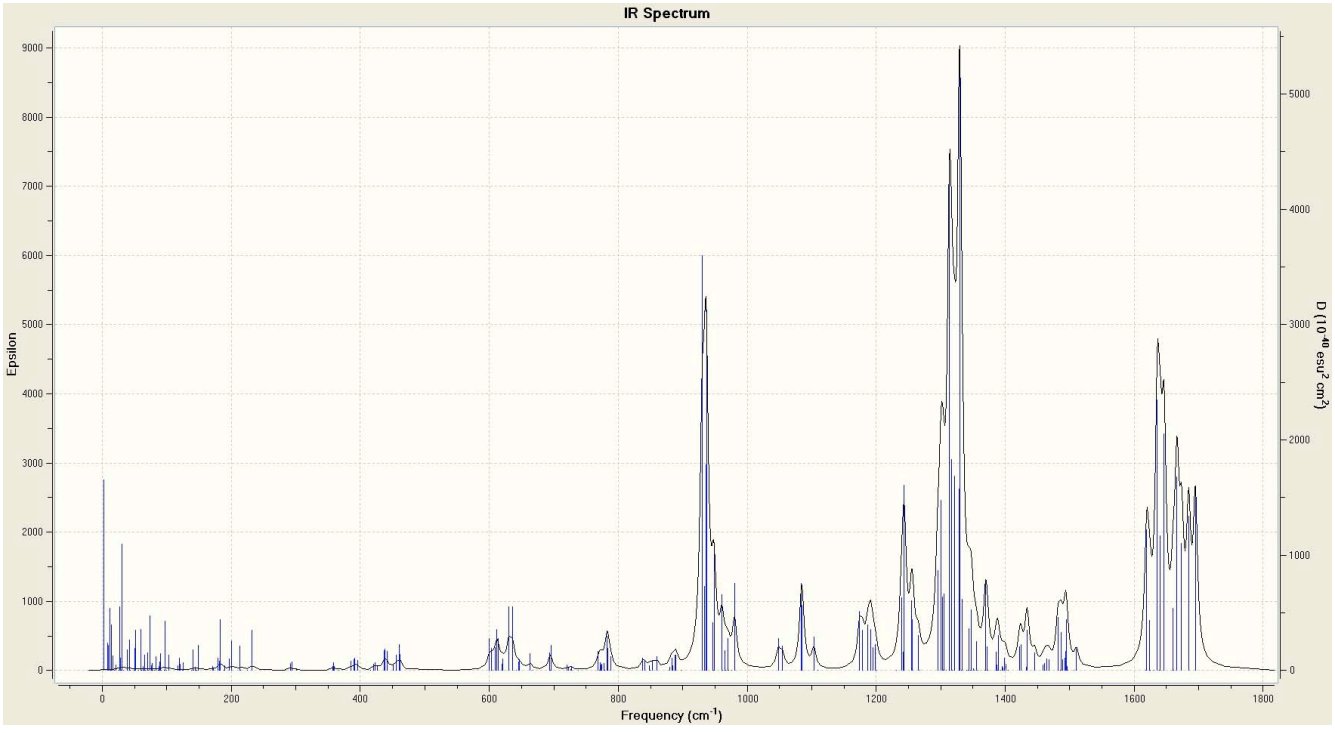

Figure 8. IR intensity as a function of frequency calculated using DFT B3LYP/6-311G(2d,2p) for five-molecule cluster of β-HMX according to frozen phonon approximation.

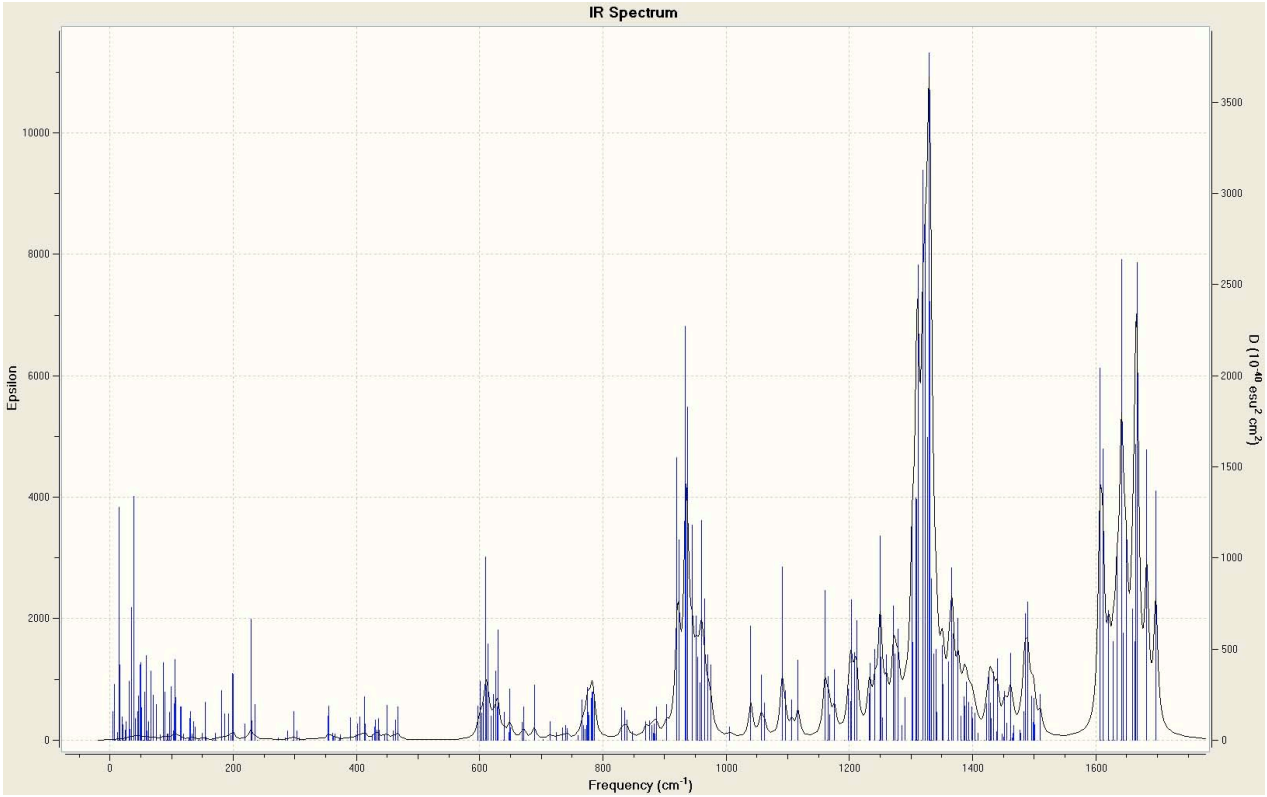

Figure 9. IR intensity as a function of frequency calculated using DFT B3LYP/6-311G(2d,2p) for seven-molecule cluster of β–HMX according to frozen phonon approximation.

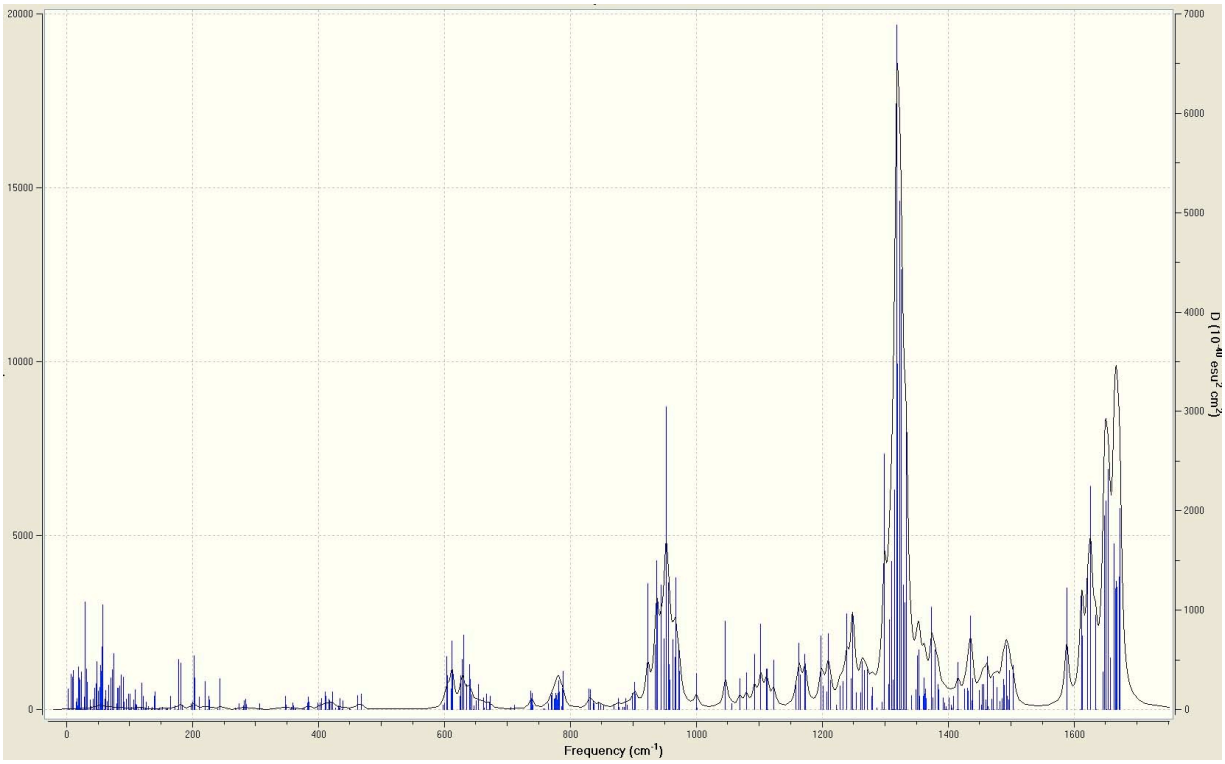

Figure 10. IR intensity as a function of frequency calculated using DFT B3LYP/6-311G(2d,2p) for nine-molecule cluster of β–HMX according to frozen phonon approximation.

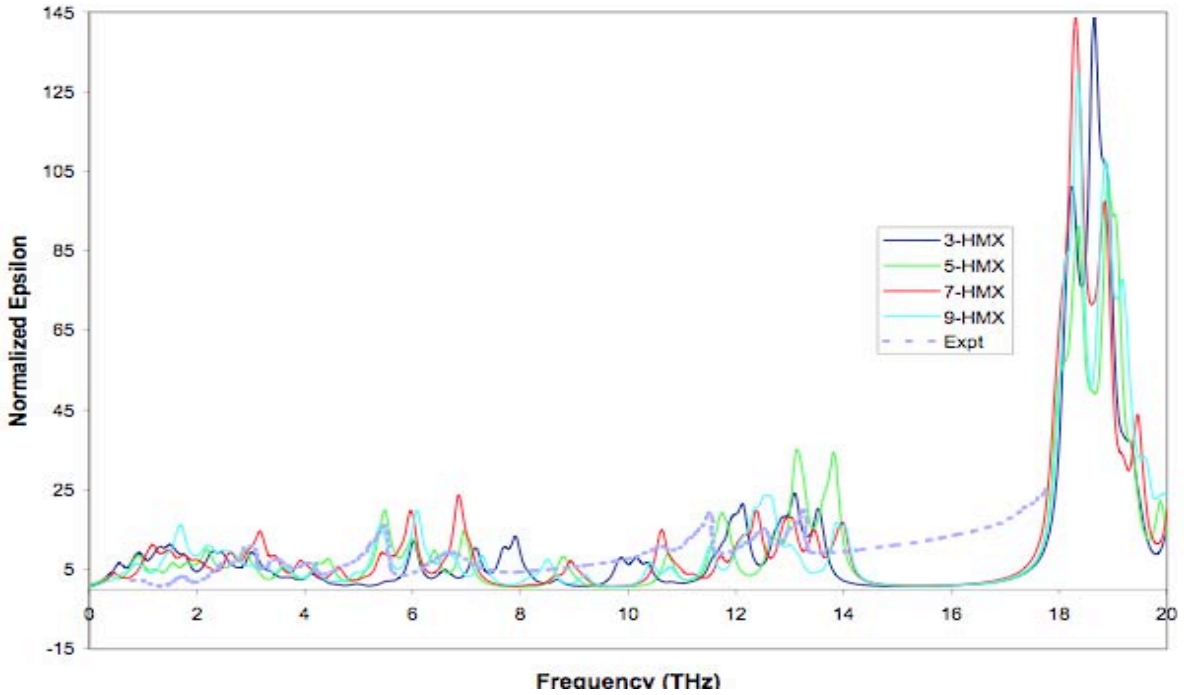

Figure 11(A). Qualitative comparison of DFT calculated spectra for 3-, 5-, 7- and 9-molecule clusters of β-HMX and experimentally measured spectrum for dielectric response of bulk lattice [20,21].

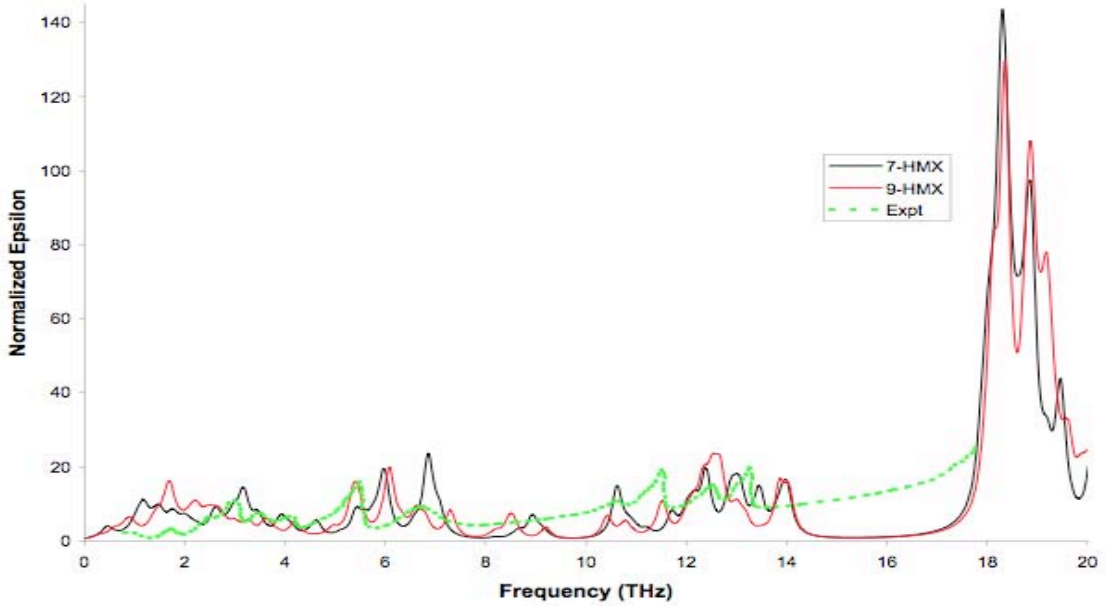

Figure 11(B). Qualitative comparison of DFT calculated spectra for 7- and 9-molecule clusters of β-HMX and experimentally measured spectrum for dielectric response of bulk lattice [20].

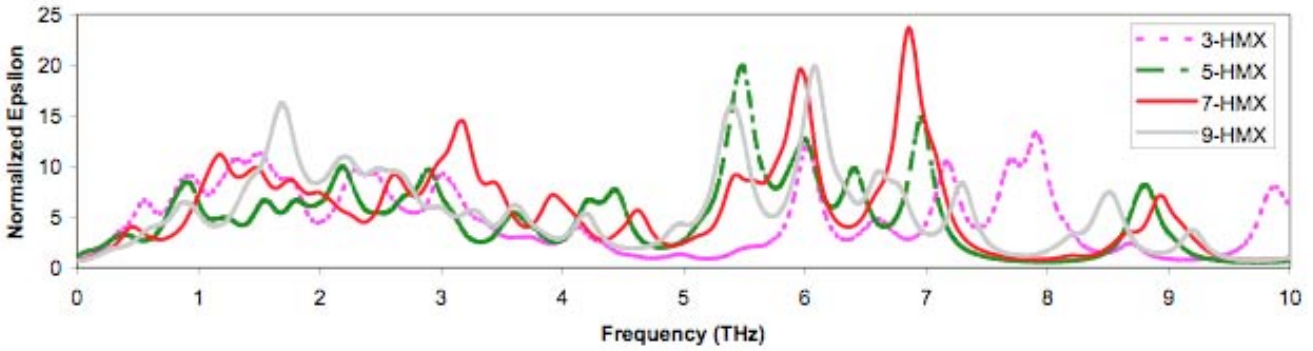

Figure 11(C). Qualitative comparison of DFT calculated spectra for 3-, 5-, 7- and 9-molecule clusters of β-HMX.

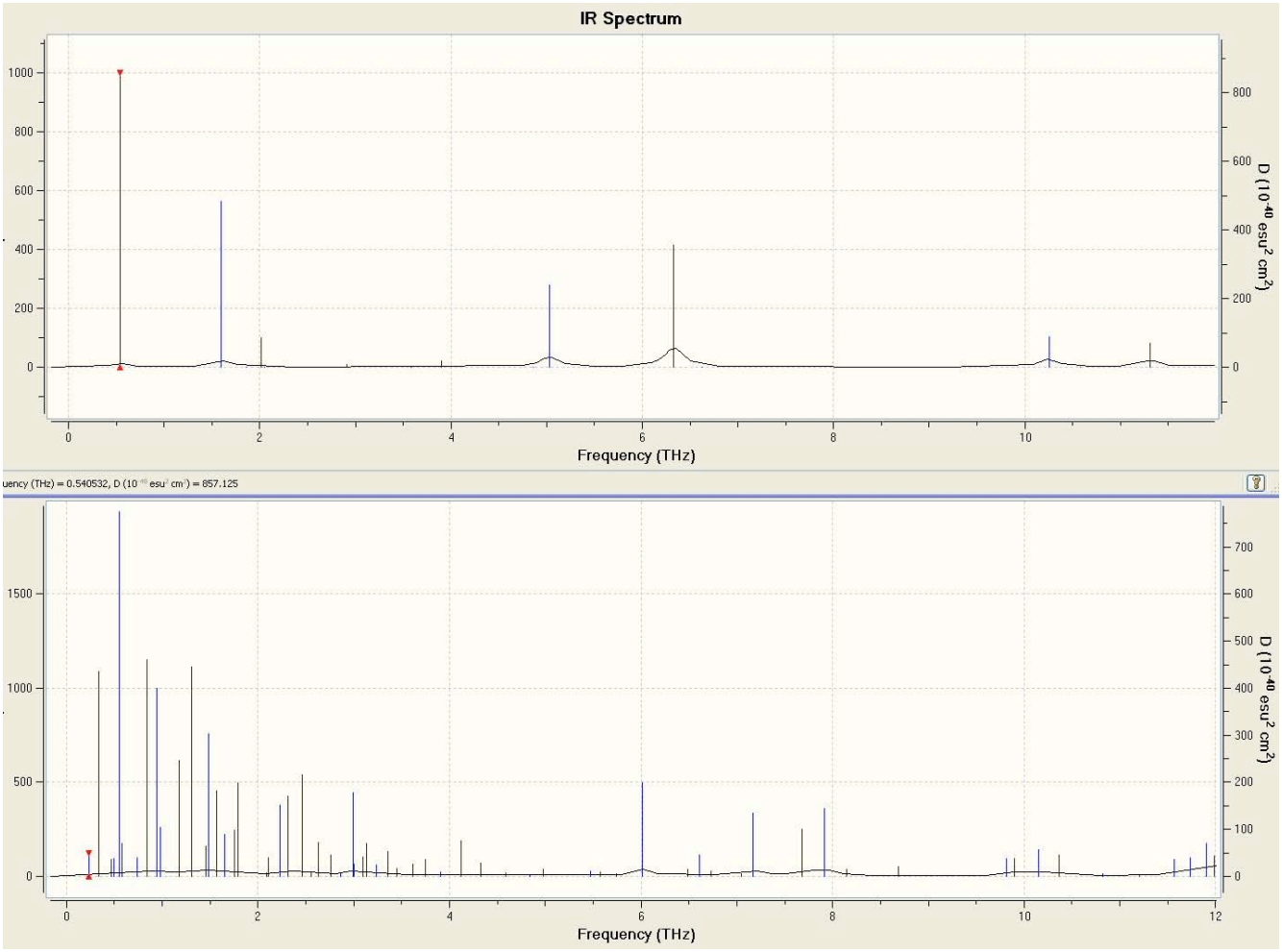

Figure 12(A). Comparison of discrete spectra for single isolate molecule and 3-molecule cluster of β-HMX.

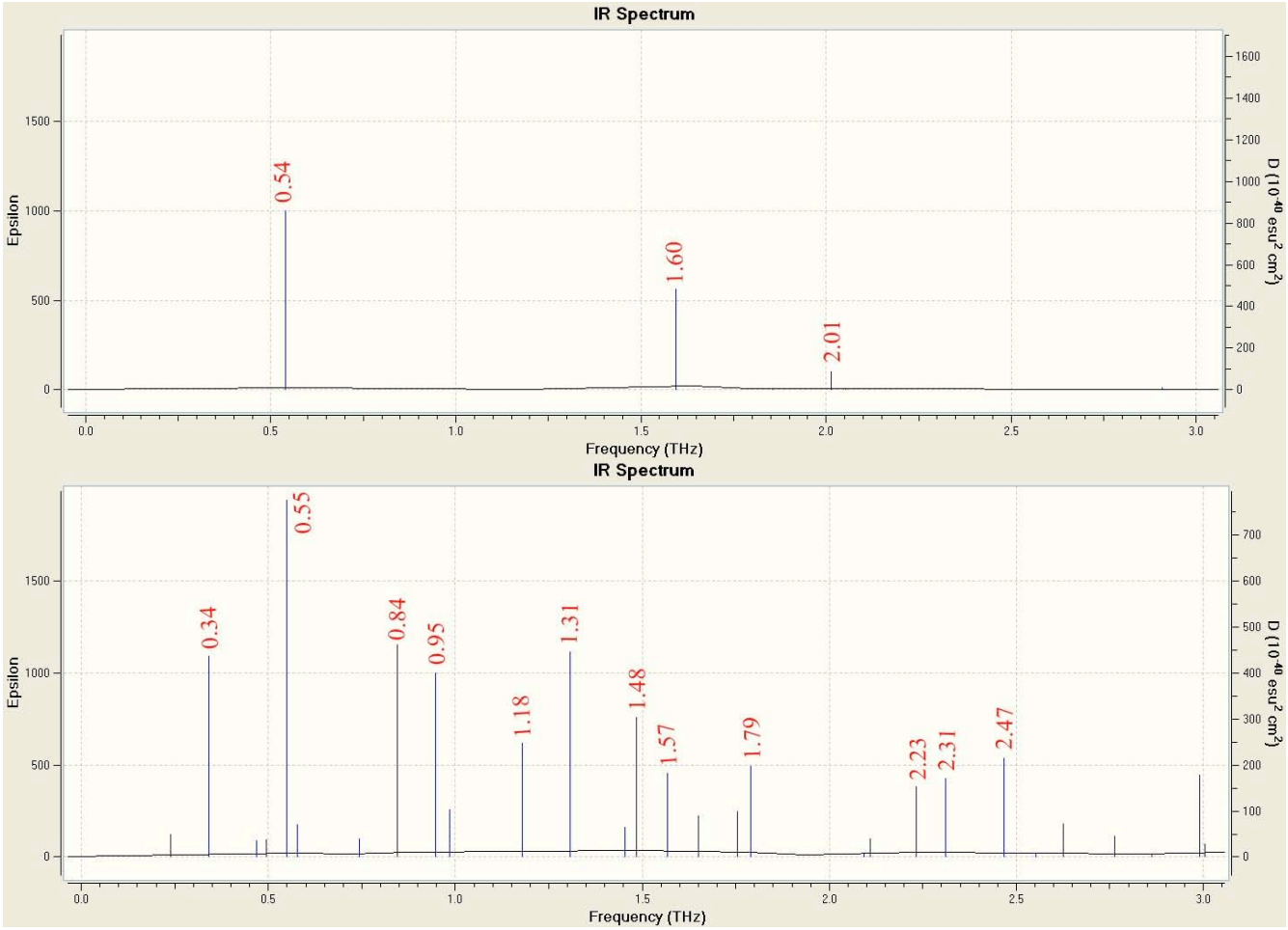

Figure 12(B). Comparison of discrete spectra for single isolate molecule and 3-molecule cluster of β-HMX.

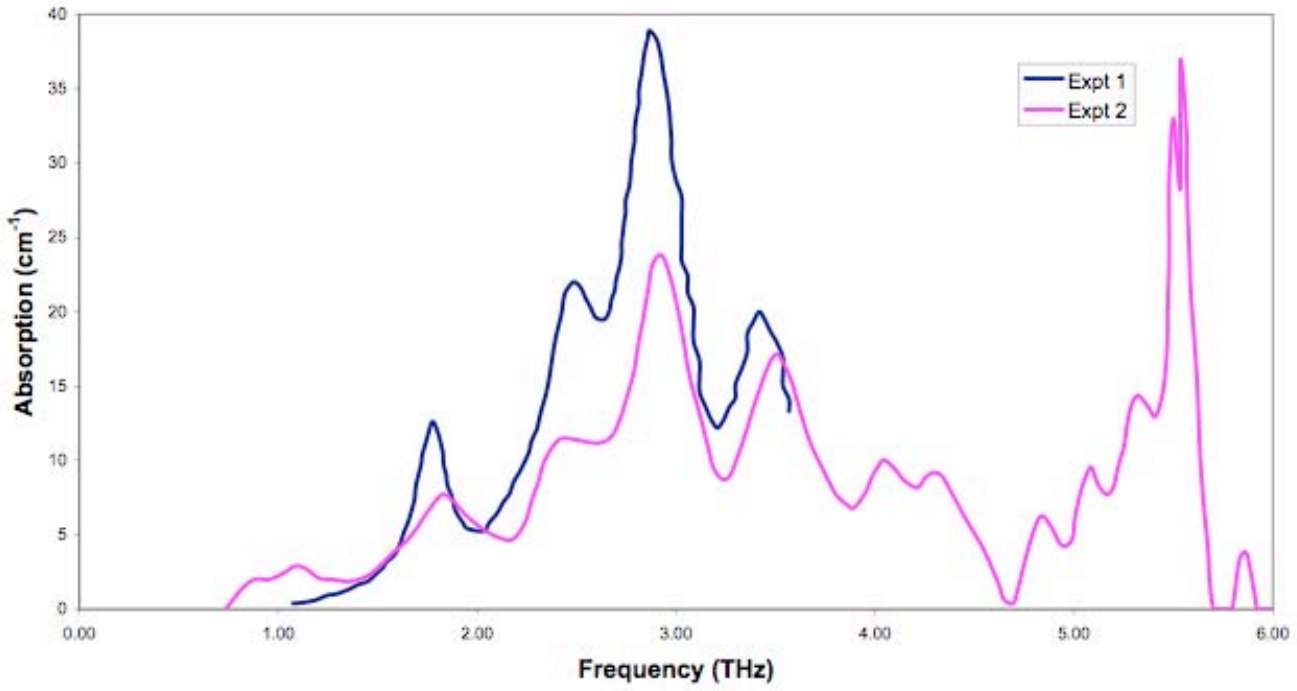

Figure 13. Experimentally measured absorption spectra for β–HMX (see Expt 1:[24] and Expt 2:[22]).

Conclusion

The calculations of ground state resonance structure associated with molecular clusters of β–HMX using DFT are meant to serve as reasonable estimates of molecular level response characteristics, providing interpretation of dielectric response features, for subsequent adjustment relative to experimental measurements and molecular structure theory.

Acknowledgement

This work was supported by the Office of Naval Research.

References

[1] M. J. Frisch, G. W. Trucks, H. B. Schlegel, G. E. Scuseria, M. A. Robb, J. R. Cheeseman, G. Scalmani, V. Barone, B. Mennucci, G. A. Petersson, H. Nakatsuji, M. Caricato, X. Li, H. P. Hratchian, A. F. Izmaylov, J. Bloino, G. Zheng, J. L. Sonnenberg, M. Hada, M. Ehara, K. Toyota, R. Fukuda, J. Hasegawa, M. Ishida, T. Nakajima, Y. Honda, O. Kitao, H. Nakai, T. Vreven, J. A. Montgomery, Jr., J. E. Peralta, F. Ogliaro, M. Bearpark, J. J. Heyd, E. Brothers, K. N. Kudin, V. N. Staroverov, R. Kobayashi, J. Normand, K. Raghavachari, A. Rendell, J. C. Burant, S. S. Iyengar, J. Tomasi, M. Cossi, N. Rega, J. M. Millam, M. Klene, J. E. Knox, J. B. Cross, V. Bakken, C. Adamo, J. Jaramillo, R. Gomperts, R. E. Stratmann, O. Yazyev, A. J. Austin, R. Cammi, C. Pomelli, J. W. Ochterski, R. L. Martin, K. Morokuma, V. G. Zakrzewski, G. A. Voth, P. Salvador, J. J. Dannenberg, S. Dapprich, A. D. Daniels, Ö. Farkas, J. B. Foresman, J. V. Ortiz, J. Cioslowski, and D. J. Fox, Gaussian 09, Revision A.1, Gaussian, Inc., Wallingford CT, 2009.

[2] A. Frisch, M. J. Frisch, F. R. Clemente and G. W. Trucks, Gaussian 09 User's Reference, pp105-106 (2009)

[3] P. Hohenberg and W. Kohn, "Inhomogeneous Electron Gas" Phys. Rev. **136**, B864, (1964).

[4] W. Kohn and L. J. Sham, "Self-Consistent Equations Including Exchange and Correlation Effects" Phys. Rev. **140**, A1133 (1965).

[5] R. O. Jones and O. Gunnarsson, "The density functional formalism, its applications and prospects" Rev. Mod. Phys. **61**, 689 (1989).

[6] W. W. Hager and H. Zhang, "A survey of nonlinear conjugate gradient methods," Pacific J. Optim., 2, p. 35-58 (2006).

[7] R. M. Martin, *Electronic Structures Basic Theory and Practical Methods*, Cambridge University Press, Cambridge 2004, p. 25.

[8] E. B. Wilson, J. C. Decius and P. C. Cross, *Molecular Vibrations* (McGraw-Hill, New York, 1955).

[9] J. W. Ochterski, "Vibrational Analysis in Gaussian," help@gaussian.com, 1999.

[10] C. A. D. Roeser and E. Mazur, "Light-Matter Interactions on Femtosecond Time Scale" in *Frontiers of Optical Spectroscopy*, eds. B. Di Bartolo and O. Forte, NATO Science Series v. 168 p. 29, Kluwer Academic Publishers, Dordrecht – Norwell, 2005; C. F. Bohren and D. R. Huffman, *Absorption and Scattering of Light by Small Particles* (Wiley-VCH Verlag, Weinheim, 2004).

[11] A. Shabaev, S. G. Lambrakos, N. Bernstein, V. L. Jacobs, D. Finkenstadt, "A General Framework for Numerical Simulation of IED-Detection Scenarios using Density Functional Theory and THz Spectra," Applied Spectroscopy, **65**, 409-416 (2011).

[12] A. D. Becke, "Density-functional Thermochemistry. III. The Role of Exact Exchange", *J. Chem. Phys.* **98**, 5648-5652 (1993).

[13] B. Miehlich, A. Savin, H. Stoll and H. Preuss, "Results of Obtained with the Correlation Energy

Density Functionals of Becke and Lee, Yang and Parr", Chem. *Phys. Lett.* **157**, 200-206 (1989).

[14] A. D. McLean and G. S. Chandler, "Contracted Gaussian-basis sets for molecular calculations. 1. 2nd row atoms, Z=11-18," *J. Chem. Phys.*, **72** 5639-48 (1980).

[15] T. Clark, J. Chandrasekhar, G. W. Spitznagel and P. V. R. Schleyer, "Efficient diffuse function-augmented basis-sets for anion calculations. 3. The 3-21+G basis set for 1st-row elements, Li-F," *J. Comp. Chem.*, **4** 294-301, (1983).

[16] M. J. Frisch, J. A. Pople and J. S. Binkley, "Self-Consistent Molecular Orbital Methods. 25. Supplementary Functions for Gaussian Basis Sets," *J. Chem. Phys.*, **80** (1984) 3265-69.

[17] C. S. Choi and H. P. Boutin, " *A Study of the Crystal Structure of* β*–Cyclotetramethylene Tetranitramine by Neutron Diffraction*," Acta Cryst. (1970) B26, 1235-1240.

[18] P. F. Eiland and R. Z. Pepinsky, Kristallogr. (1955) 106, 273.

[19] I. J. Bruno, J. C. Cole, P. R. Edgington, M. K. Kessler, C. F. Macrae, P.McCabe, J. Pearson and R. Taylor, *"New software for seaching the Cambridge Structural Database and visualizing crystal structures"*, Acta Cryst. (2002) B58, 389-397.

[20] T. Lo, I. S. Gregory, C. Baker, P.F. Taday, W.R. Tribe, M.C. Kemp, "The very far-infrared spectra of energetic materials and possible confusion materials using terahertz pulsed spectroscopy," Vibrational Spectroscopy, 42 (2006) 243-246.

[21] M.R. Leahy-Hoppa, M.J. Fitch, R. Osiander, "Terahertz spectroscopy techniques for explosives detection,' Anal. Bioanal. Chem., **395,** 247 (2009).

[22] M.R. Leahy-Hoppa, M.J. Fitch, X. Zheng, L.M. Hayden, R. Osiander, "Wideband terahertz spectroscopy of explosives,' Chem. Phys. Lett., **434,** 227 (2007).

[23] D. G. Allis, D. A. Prokhorova, T. M. Korter, "Solid-State Modeling of the Terahertz Spectrum of the High Explosive HMX," J. Phys. Chem. A., 110, 1951-1959 (2006).

[24] J. Hooper, E. Mitchell, C. Konek and J. Wilkinson, "Terahertz optical properties of the high explosive β–HMX," Chem. Phys. Lett., **467**, 309 (2009).

APPENDIX 1

Table A1. Oscillation frequencies and IR intensities for 9-Molecule Cluster of β–HMX.

Frequency (cm^{-1})	IR Intebsity (km/mol)	Frequency (cm^{-1})	IR Intebsity (km/mol)	Frequency (cm^{-1})	IR Intebsity (km/mol)
3.0589	0.1609	44.8527	2.4087	91.7931	0.0000
4.8222	0.0000	46.5996	3.0660	94.4437	2.5236
4.9342	0.0137	46.6736	0.0000	94.4674	0.0000
7.3335	0.6538	47.8356	5.7805	99.0039	3.8028
9.2848	0.0000	49.9196	0.0000	99.1579	0.0000
9.8937	0.8044	50.0891	2.3728	100.3894	3.9776
9.9664	0.0000	52.0946	0.0000	100.7604	0.0000
10.9415	1.0889	53.0528	2.9306	102.4655	0.0000
14.4391	0.0000	54.4141	6.0855	102.7112	0.4959
15.0600	0.2733	54.6853	0.0000	106.2763	2.6303
15.5835	0.0000	54.8855	5.3117	107.2620	0.0000
16.3880	0.4733	54.9397	0.0000	109.1793	0.0000
16.8100	0.0000	56.6874	0.0000	109.1833	5.4600
17.4681	0.0000	56.9185	9.0422	109.8157	0.0000
17.7853	0.1600	57.2134	15.0807	109.9017	1.4169
18.2657	0.0000	57.879	0.0000	111.4961	1.2386
18.6292	1.9965	59.8875	0.0000	111.8350	0.0000
19.7876	1.5819	60.5383	1.5491	113.3649	0.0000
20.0087	0.0000	61.1305	0.0000	113.4881	0.1755
20.9188	1.5587	62.61	3.0158	118.9086	0.5832
21.3477	0.0000	64.7568	1.3818	118.9166	0.0000
22.9352	0.1041	65.1342	0.0000	119.8885	7.9987
23.1584	0.0000	67.1805	4.1230	119.9646	0.0000
24.1788	2.3126	69.7855	0.0000	122.0718	4.0225
25.3158	0.0000	70.5773	0.0000	122.0895	0.0000
25.6744	0.0000	70.703	5.6330	124.2173	0.0000
27.4832	0.0000	72.5264	7.3171	125.3255	0.1409
28.1634	0.8938	72.8601	0.0000	126.9006	2.3012
28.4577	0.6056	74.2589	0.0000	126.9808	0.0000
28.6072	0.0000	75.3011	10.6928	129.5798	0.9385
28.9844	7.8511	79.3039	0.0000	129.7329	0.0000
30.8694	0.0000	79.3567	1.2210	135.0062	0.0000
31.8306	3.2624	80.3723	0.0000	135.7114	0.7794
32.8765	0.0000	80.8141	4.3703	139.3064	0.0000
33.4881	2.3233	82.2753	0.0000	139.5810	4.6199
35.2329	0.0000	82.48	4.4585	140.0262	0.0000
38.0644	0.9300	83.969	5.0222	140.2016	6.2496
38.4248	0.0000	84.7009	0.0000	145.0526	0.0000
39.0128	0.3030	87.3554	7.6747	145.8394	0.2845
41.4919	0.0000	90.0183	0.0000	146.0603	0.0000
42.0202	0.0000	90.3001	7.4628	146.3392	0.0844
42.2045	1.1368	90.4423	0.0000	146.4261	0.0000
44.4634	0.0000	91.477	1.7809	147.3312	0.3254

Frequency (cm^{-1})	IR Intebsity (km/mol)	Frequency (cm^{-1})	IR Intebsity (km/mol)	Frequency (cm^{-1})	IR Intebsity (km/mol)
150.2794	0.0000	282.3828	0.0000	416.6851	9.4722
152.7555	0.8129	282.3919	6.5274	416.7334	0.0000
152.7661	0.0000	284.8366	7.6799	417.1550	10.7234
157.6321	0.3079	284.8732	0.0000	417.2148	0.0000
158.7700	0.0000	285.6078	0.0000	418.1298	9.6942
160.9158	0.5915	285.6123	3.5977	418.3102	0.0000
165.0031	0.0000	306.4664	0.0000	419.9929	0.0000
165.0891	5.6563	306.4984	3.8995	419.9983	6.9950
172.1161	0.0000	307.0307	0.0000	422.7608	16.2783
172.1240	1.4707	307.1653	4.3422	422.9878	0.0000
175.5053	0.0000	310.2005	0.0000	422.9906	18.8363
178.3599	22.7225	347.2119	11.4797	426.9904	0.0000
178.3961	0.0000	347.2169	0.0000	427.1127	1.6427
181.7942	21.1974	348.5020	0.0000	431.5656	0.0000
183.5498	0.0000	348.5033	4.2188	431.7640	3.9142
183.8341	2.2245	356.3596	0.0000	432.4742	0.0000
197.4803	2.8143	356.4486	2.0605	432.5052	1.8774
197.9040	0.0000	359.7182	5.8980	434.5371	12.0080
200.7045	0.0000	359.7735	0.0000	434.5428	0.0000
200.7918	3.6363	360.3010	3.5521	438.1680	0.0000
202.4904	0.0000	363.0656	0.0000	439.4543	9.7152
202.5388	27.6179	364.5449	0.0000	449.9553	2.0814
203.4812	16.3953	364.5477	1.4170	450.1586	0.0000
203.8936	0.0000	376.2069	0.5186	462.0350	15.9271
210.6395	0.0000	376.2205	0.0000	462.0426	0.0000
210.6694	6.8297	377.7119	0.6738	462.2056	16.2903
220.2040	15.7196	377.7154	0.0000	462.2126	0.0000
223.8720	0.0000	382.7746	6.2763	467.7770	0.0000
225.4227	7.4225	382.8343	0.0000	467.8270	11.3606
226.8692	0.0000	384.3813	0.0000	468.5008	0.0000
227.0515	5.6344	384.3905	12.2365	468.5083	18.2266
230.9002	0.0000	384.8943	6.8712	598.4034	0.0000
240.5131	0.4365	399.0401	6.4743	598.4035	7.0967
240.5234	0.0000	399.0403	0.0000	600.1239	0.0000
243.4292	0.0000	402.5414	0.0000	600.1301	9.6544
243.4307	19.1601	402.5434	7.1401	600.7519	0.0000
268.4504	0.0000	405.0952	11.4173	600.7657	8.8609
268.4514	0.8302	405.1642	0.0000	603.7589	0.0000
273.3699	0.0000	410.6773	18.7025	603.8746	80.6165
273.4493	4.2937	410.7332	0.0000	604.9462	0.0000
280.0068	0.0000	412.4351	13.4697	604.9942	51.3324
281.2317	2.4458	412.4439	0.0000	605.3075	0.0000
281.3427	0.0000	414.2618	0.0000	611.0852	31.8223

Frequency (cm^{-1})	IR Intebsity (km/mol)	Frequency (cm^{-1})	IR Intebsity (km/mol)	Frequency (cm^{-1})	IR Intebsity (km/mol)
611.5164	0.0000	711.2124	7.7231	782.1045	56.6044
611.5545	95.3862	736.3339	0.0000	782.1138	0.0000
612.5518	0.0000	737.4395	34.6371	782.2184	0.0000
612.5962	105.8302	737.6298	0.0000	782.2895	34.9943
612.8365	61.0344	738.8604	18.8301	782.3912	0.0000
613.1074	0.0000	738.8727	0.0000	786.6030	5.2578
625.3357	0.0000	739.0037	29.8386	786.8790	0.0000
625.3617	21.0451	739.1523	0.0000	786.9333	42.5699
626.3601	0.0000	740.2820	8.7642	787.8560	0.0000
626.3854	53.8156	740.5513	0.0000	788.4525	76.2665
628.3036	0.0000	756.5863	1.0489	829.7294	0.0000
628.4369	79.8878	756.6723	0.0000	829.8467	42.8804
630.3791	117.9702	759.0960	0.0000	832.0939	0.0000
630.4501	0.0000	759.1051	1.9706	832.1419	41.4107
635.9279	39.9878	765.3854	11.3151	836.2425	0.0000
635.9463	0.0000	769.5468	0.0000	836.2615	18.1690
639.6649	72.8626	769.6079	8.6775	837.3795	0.0000
640.6799	0.0000	769.7348	0.0000	838.2496	12.1550
640.8135	49.2547	770.1497	26.6240	844.4608	0.0000
640.9916	0.0000	771.2266	31.4257	844.5041	15.3446
643.6895	0.0000	771.2986	0.0000	847.7972	11.1952
643.7110	24.5166	774.0945	0.0000	847.8067	0.0000
646.5415	0.0000	774.5456	20.9255	848.7909	11.1697
646.5493	5.5682	774.5821	0.0000	848.7928	0.0000
646.8431	0.0000	774.9096	17.5092	852.9426	9.8742
646.8494	6.6298	774.9189	0.0000	852.9513	0.0000
650.6717	14.2679	775.3863	0.0000	869.0932	10.6009
650.6779	0.0000	775.3936	21.4217	869.2198	0.0000
654.4732	41.5640	776.9600	31.6935	876.4321	23.7545
654.5388	0.0000	776.9600	0.0000	876.5303	0.0000
662.2782	19.3558	777.5568	7.0415	877.7376	0.0000
663.6385	0.0000	777.5631	0.0000	877.7381	4.5336
663.6734	2.8586	777.9254	0.0000	883.5334	5.0753
667.1950	0.0000	777.9262	10.4322	883.5506	0.0000
667.2235	26.5620	778.0795	27.4816	885.7210	5.5972
669.3438	0.0000	778.0816	0.0000	885.7272	0.0000
672.0276	0.0000	779.2884	19.0294	888.0072	24.6911
672.0314	12.4935	780.7926	0.0000	888.0948	0.0000
672.5618	0.0000	780.8256	16.8607	890.2421	10.1887
672.5752	22.9742	781.0393	32.5611	898.3731	0.0000
705.5053	3.5611	781.0593	0.0000	898.4359	37.0542
705.5429	0.0000	781.2754	0.0000	901.1130	0.0000
711.2000	0.0000	781.2781	25.2844	902.4019	61.9739

Frequency (cm^{-1})	IR Intebsity (km/mol)	Frequency (cm^{-1})	IR Intebsity (km/mol)	Frequency (cm^{-1})	IR Intebsity (km/mol)
902.4172	0.0000	1069.1399	0.0000	1239.3871	300.7010
903.2393	35.3158	1069.1497	82.9367	1246.3226	0.0000
903.2488	0.0000	1079.6486	100.4909	1246.3459	97.1055
923.0291	0.0000	1079.6750	0.0000	1248.2227	0.0000
923.1269	293.6896	1092.7532	0.0000	1248.4575	287.7837
934.9380	0.0000	1092.7867	153.0708	1248.8077	296.2883
934.9842	152.8568	1102.6061	0.0000	1249.1895	0.0000
937.3676	0.0000	1102.6500	237.1637	1253.8058	0.0000
937.4529	352.7703	1111.0460	113.6086	1253.8127	53.3507
938.2572	258.6206	1111.6967	0.0000	1261.2681	54.6568
938.5605	0.0000	1113.2761	114.6659	1261.2870	0.0000
944.1770	0.0000	1113.3680	0.0000	1263.1945	0.0000
944.3683	297.4993	1123.2775	140.1602	1263.2977	151.9045
948.6611	170.2016	1123.3206	0.0000	1266.7871	124.1344
949.3053	0.0000	1158.5103	0.0000	1266.8239	0.0000
951.8024	0.0000	1158.5247	76.6950	1271.4272	0.0000
952.0880	727.4727	1163.4269	195.6650	1271.5337	127.4992
952.7322	186.9147	1163.4297	0.0000	1278.4930	0.0000
953.0494	0.0000	1165.1295	0.0000	1278.6663	42.2970
956.2035	305.0435	1165.1871	101.3553	1280.3604	70.7683
956.2685	0.0000	1171.9982	163.1103	1280.5410	0.0000
956.7171	108.7616	1172.2203	0.0000	1287.2513	0.0000
958.5111	0.0000	1174.0367	134.8576	1287.2531	4.6827
958.7058	72.1648	1197.9561	0.0000	1294.8718	24.8197
962.4360	0.0000	1198.2711	222.1726	1294.9034	0.0000
962.8742	169.7053	1198.4749	0.0000	1297.9899	0.0000
963.8116	0.0000	1202.0476	71.0994	1299.0874	837.7520
966.0670	127.9082	1202.2013	0.0000	1306.0563	82.1228
966.1346	0.0000	1207.6990	54.0489	1306.1112	0.0000
967.6316	322.2196	1207.7601	0.0000	1306.6349	0.0000
968.1927	0.0000	1209.7051	0.0000	1306.6683	295.5881
970.0813	0.0000	1209.7445	231.6095	1310.3438	0.0000
972.3522	152.4676	1213.1711	0.0000	1310.6219	489.5182
972.5794	0.0000	1213.2046	90.1670	1311.5242	0.0000
973.6731	94.6109	1222.9182	0.0000	1312.5815	96.8039
1000.3992	0.0000	1223.1240	13.4127	1313.9323	0.0000
1000.4125	91.1893	1223.6454	0.0000	1314.8007	727.4005
1001.3819	0.0000	1227.9927	59.2899	1315.7437	0.0000
1001.3843	3.0429	1228.0114	0.0000	1318.4603	2276.8538
1046.5330	0.0000	1228.6572	0.0000	1319.6299	1150.7643
1046.5619	232.8664	1228.6577	73.2388	1319.8845	0.0000
1056.3582	0.0000	1233.7606	87.9568	1322.6234	0.0000
1056.3624	16.5189	1239.1147	0.0000	1322.9297	1696.4060

Frequency (cm^{-1})	IR Intebsity (km/mol)	Frequency (cm^{-1})	IR Intebsity (km/mol)	Frequency (cm^{-1})	IR Intebsity (km/mol)
1324.9562	0.0000	1385.0790	43.4204	1459.6213	12.8888
1325.7565	1471.3215	1391.8134	40.7520	1460.7495	0.0000
1327.7542	0.0000	1391.8341	0.0000	1460.7532	34.1601
1328.7046	417.9261	1394.1884	24.5670	1461.4714	0.0000
1331.6687	358.4903	1395.3529	0.0000	1462.3639	194.7866
1332.2094	0.0000	1397.4808	11.7323	1463.5115	0.0000
1333.4880	0.0000	1397.4819	0.0000	1463.6318	11.1883
1333.7661	1021.2266	1397.5297	10.6667	1466.5480	0.0000
1333.9757	173.9448	1397.7893	0.0000	1469.4231	37.3948
1341.5800	0.0000	1401.4248	42.2661	1469.6011	0.0000
1341.5920	47.6440	1401.4260	0.0000	1472.4415	124.6282
1349.4401	0.0000	1405.5529	0.0000	1472.5033	0.0000
1349.5316	66.8270	1405.5552	16.7833	1477.8409	58.6643
1351.0509	0.0000	1406.1211	4.5206	1478.0828	0.0000
1351.9644	183.5376	1406.2627	0.0000	1478.2845	81.9909
1353.3383	0.0000	1408.1694	0.0000	1479.7701	0.0000
1353.4001	20.2769	1408.2173	48.3013	1482.5077	31.0708
1353.7863	0.0000	1415.1129	0.0000	1482.5778	0.0000
1354.1031	0.0000	1416.1711	169.0238	1485.9283	0.0000
1354.2795	204.4144	1416.4220	0.0000	1486.1113	42.3127
1355.1298	0.0000	1426.1147	74.6876	1486.2852	35.1559
1355.1342	45.6055	1426.1388	0.0000	1486.2924	0.0000
1360.9619	0.0000	1431.1497	0.0000	1487.4209	0.0000
1360.9780	44.6298	1431.1759	78.1278	1487.7068	112.8795
1361.6737	107.9211	1431.9467	65.9690	1487.7466	0.0000
1361.6866	0.0000	1432.0540	0.0000	1489.3242	91.0170
1362.6187	0.0000	1432.1406	0.0000	1489.3987	0.0000
1362.8113	53.8569	1432.1448	28.2325	1492.5964	242.3142
1363.7267	0.0000	1435.4635	14.7927	1492.6479	0.0000
1363.7307	69.8919	1435.6086	0.0000	1494.2771	38.6828
1365.4056	37.3478	1435.7069	338.0437	1494.4747	0.0000
1369.4180	0.0000	1435.8829	0.0000	1494.6195	51.2859
1373.8313	0.0000	1437.5424	31.8616	1496.3198	0.0000
1373.9529	354.5626	1437.5452	0.0000	1496.3615	36.5042
1375.8939	40.3350	1438.9015	111.9497	1497.5397	0.0000
1375.9177	0.0000	1449.1140	0.0000	1497.7275	40.0383
1378.9482	208.0525	1449.1392	68.8937	1498.0544	146.9730
1379.2183	0.0000	1452.8182	16.2419	1498.0574	0.0000
1383.6650	0.0000	1453.8969	0.0000	1503.6014	166.6402
1383.6842	88.5264	1454.4268	91.8006	1503.6514	0.0000
1384.7758	69.1407	1456.6174	0.0000	1588.5010	487.3644
1384.9431	0.0000	1456.7140	91.5698	1588.5470	0.0000
1385.0764	0.0000	1459.5551	0.0000	1609.4855	0.0000

Frequency (cm^{-1})	IR Intebsity (km/mol)	Frequency (cm^{-1})	IR Intebsity (km/mol)	Frequency (cm^{-1})	IR Intebsity (km/mol)
1612.0302	481.8943	3095.2383	0.0000	3179.0752	0.0000
1613.0077	0.0000	3095.2388	1.5663	3179.8782	82.5672
1613.0217	300.0930	3095.4504	4.6078	3179.9458	0.0000
1622.0391	0.0000	3095.4512	0.0000	3183.6404	0.0000
1622.1224	558.7517	3097.1121	21.3954	3183.6699	116.2304
1626.1351	0.0000	3097.1160	0.0000	3185.3113	0.0000
1626.6447	915.8177	3102.2402	31.3289	3185.3289	88.3884
1634.0691	389.9972	3102.2424	0.0000	3186.5447	0.0000
1636.1240	0.0000	3105.6938	0.0000	3186.5449	12.1191
1645.9258	157.5226	3105.8640	1.8201	3193.6030	59.1381
1646.0087	0.0000	3108.1821	30.6836	3193.6133	0.0000
1648.3832	0.0000	3108.2034	0.0000	3194.7830	15.7027
1648.4786	806.7298	3114.8772	3.2888	3194.7842	0.0000
1650.3507	867.0773	3114.8801	0.0000	3196.2114	0.0000
1650.5728	0.0000	3115.7144	0.0000	3196.2146	34.9003
1652.0148	0.0000	3115.7158	5.2948	3204.8938	24.8867
1654.4449	1002.9441	3117.5549	0.0000	3204.9009	0.0000
1656.9803	0.0000	3117.5552	0.4579	3219.1714	0.0000
1657.4988	216.5820	3129.0730	1.0154	3219.1826	41.0084
1663.2891	0.0000	3129.0730	0.0000		
1663.4043	436.4607	3129.8232	11.6127		
1664.1381	0.0000	3129.8257	0.0000		
1664.1711	696.5076	3130.5049	37.6583		
1666.2166	0.0000	3130.5491	0.0000		
1666.3400	507.7381	3130.7036	0.0000		
1667.6038	0.0000	3130.7039	3.9111		
1667.6705	540.2437	3149.6797	0.0000		
1668.6038	0.0000	3149.6799	2.1275		
1668.9050	516.6068	3155.7021	13.2500		
1671.8771	0.0000	3155.7046	0.0000		
1672.0051	558.5286	3159.5952	0.0000		
1673.0131	847.5236	3159.5967	3.1555		
1673.4744	0.0000	3164.7078	1.7978		
3081.3857	0.0000	3164.7078	0.0000		
3081.3862	4.8444	3170.9243	6.9908		
3085.2014	4.1627	3171.0217	0.0000		
3085.2017	0.0000	3173.0881	0.0000		
3086.2803	21.5776	3173.0894	15.0731		
3086.2822	0.0000	3173.4294	0.0000		
3088.2292	0.0000	3173.4299	6.3130		
3088.2317	16.6014	3174.9609	0.0000		
3093.5842	0.0000	3174.9624	17.0108		
3093.5916	23.2331	3179.0691	34.8096		